AEDC-TR-73-194

cy. 4

JUN 4 1979
APR 3 1981
APR 13 1988

STUDIES OF BOUNDARY-LAYER TRANSITION ON AEROBALLISTIC RANGE MODELS

J. Leith Potter
ARO, Inc.

VON KÁRMÁN GAS DYNAMICS FACILITY
ARNOLD ENGINEERING DEVELOPMENT CENTER
AIR FORCE SYSTEMS COMMAND
ARNOLD AIR FORCE STATION, TENNESSEE 37389

May 1974

Final Report for Period July 1, 1971 – June 30, 1973

Approved for public release; distribution unlimited.

Property of U. S. Air Force
AEDC LIBRARY

Prepared for

ARNOLD ENGINEERING DEVELOPMENT CENTER
AIR FORCE SYSTEMS COMMAND
ARNOLD AIR FORCE STATION, TENNESSEE 37389

NOTICES

When U. S. Government drawings specifications, or other data are used for any purpose other than a definitely related Government procurement operation, the Government thereby incurs no responsibility nor any obligation whatsoever, and the fact that the Government may have formulated, furnished, or in any way supplied the said drawings, specifications, or other data, is not to be regarded by implication or otherwise, or in any manner licensing the holder or any other person or corporation, or conveying any rights or permission to manufacture, use, or sell any patented invention that may in any way be related thereto.

Qualified users may obtain copies of this report from the Defense Documentation Center.

References to named commercial products in this report are not to be considered in any sense as an endorsement of the product by the United States Air Force or the Government.

APPROVAL STATEMENT

This technical report has been reviewed and is approved.

Elton R. Thompson

ELTON R. THOMPSON
Research and Development
Division
Directorate of Technology

Robert O. Dietz

ROBERT O. DIETZ
Director of Technology

UNCLASSIFIED

SECURITY CLASSIFICATION OF THIS PAGE *(When Data Entered)*

REPORT DOCUMENTATION PAGE		READ INSTRUCTIONS BEFORE COMPLETING FORM
1. REPORT NUMBER AEDC-TR-73-194	2. GOVT ACCESSION NO.	3. RECIPIENT'S CATALOG NUMBER
4. TITLE *(and Subtitle)* STUDIES OF BOUNDARY-LAYER TRANSITION ON AEROBALLISTIC RANGE MODELS		5. TYPE OF REPORT & PERIOD COVERED Final Report - July 1, 1971 to June 30, 1973 6. PERFORMING ORG. REPORT NUMBER
7. AUTHOR*(s)* J. Leith Potter, ARO, Inc.		8. CONTRACT OR GRANT NUMBER*(s)*
9. PERFORMING ORGANIZATION NAME AND ADDRESS Arnold Engineering Development Center Air Force Systems Command Arnold AF Station, TN 37389		10. PROGRAM ELEMENT, PROJECT, TASK AREA & WORK UNIT NUMBERS Program Elements 65802F and 61102F
11. CONTROLLING OFFICE NAME AND ADDRESS Arnold Engineering Development Center (XON), Air Force Systems Command Arnold AF Station, TN 37389		12. REPORT DATE May 1974 13. NUMBER OF PAGES 47
14. MONITORING AGENCY NAME & ADDRESS*(if different from Controlling Office)*		15. SECURITY CLASS. *(of this report)* UNCLASSIFIED 15a. DECLASSIFICATION/DOWNGRADING SCHEDULE N/A

16. DISTRIBUTION STATEMENT *(of this Report)*

Approved for public release; distribution unlimited.

17. DISTRIBUTION STATEMENT *(of the abstract entered in Block 20, if different from Report)*

18. SUPPLEMENTARY NOTES

Available in DDC

19. KEY WORDS *(Continue on reverse side if necessary and identify by block number)*

boundary layer transition	noise
conical bodies	angle of attack
aeroballistic ranges	vibration
surface roughness	aerodynamic heating

20. ABSTRACT *(Continue on reverse side if necessary and identify by block number)*

This research was undertaken with the purpose of obtaining information on boundary-layer transition under conditions where disturbances associated with wind tunnel flows would not be present. In particular, it was an objective to learn more concerning the so-called unit Reynolds number effect which appeared in the free-flight range data previously published by the author (1968). The location of boundary-layer transition was determined from shadowgrams of nominally sharp, 4- and 10-deg semiangle cones at free-stream Mach numbers

DD FORM 1 JAN 73 1473 EDITION OF 1 NOV 65 IS OBSOLETE

UNCLASSIFIED

SECURITY CLASSIFICATION OF THIS PAGE *(When Data Entered)*

of 2.2 and 5.1 in an aeroballistic range. Static pressure was varied at near-constant range air temperature to produce unit Reynolds numbers of 0.6×10^6 to 8×10^6 per inch. Owing to constant and equal free-stream and cone skirt temperatures, the average ratio of cone wall-to-adiabatic recovery temperature was 0.5 at Mach 2.2 and 0.18 at Mach 5.1. Disturbances normally associated with wind tunnel streams were entirely absent in the free-flight range. Noise, which is believed to disturb boundary layers on models in wind tunnels under some conditions, was several orders of magnitude below typical wind tunnel levels in the area of the aeroballistic model at the time it was being photographed. The more prominent features of free-flight experimentation that may be suspected of influencing boundary-layer transition were investigated. These included (1) oscillatory motion and finite angles of attack, (2) cold-wall surface roughness at high unit Reynolds numbers, (3) vibration of the model, and (4) nonuniform (hot-tip) surface temperature. There was no evidence that any of these four special range conditions influenced the major results, but all are discussed. The data show local Reynolds number of transition increasing as approximately the 0.65 power of unit Reynolds number for both Mach numbers. Absolute levels of transitional Reynolds numbers also are practically equal for each Mach number at a given unit Reynolds number. A siren was used to provide 130 db noise with a dominant frequency of 800 Hz. This elevated the fluctuating sound pressure ratio by a factor of 200 but produced no measurable effect on transition locations. However, even this amount of noise was well below that typical of contemporary supersonic tunnels.

AFSC
Arnold AFS Tenn

PREFACE

The work reported herein was conducted at the Arnold Engineering Development Center (AEDC) under joint sponsorship of the Aerospace Research Laboratory (ARL) and AEDC, Air Force Systems Command (AFSC), under Program Element 61102F, Project 7065. The results of research presented were obtained by ARO, Inc. (a subsidiary of Sverdrup & Parcel and Associates, Inc.), contract operator of AEDC, AFSC, Arnold Air Force Station, Tennessee. The ARO Project Numbers were VW5212 and VF212, and the manuscript (ARO Control No. ARO-VKF-TR-73-130) was submitted for publication on September 20, 1973.

The help of the writer's colleagues in the Aerospace Instrumentation and the Aeroballistics Branches of the von Kármán Gas Dynamics Facility should be recognized. In particular, E. J. Sanders, R. P. Young, J. R. DeWitt, J. R. Blanks, E. E. Callens, and H. G. Harris have made specific contributions to the experimental program.

CONTENTS

Page

1.0 INTRODUCTION 5
2.0 BACKGROUND INVESTIGATIONS 6
3.0 MODELS AND RANGE SYSTEMS 11
4.0 RANGE AIR CONDITIONS 14
5.0 SOME FEATURES OF AEROBALLISTIC EXPERIMENTATION
5.1 Influence of Angle of Attack 16
5.2 Influence of Surface Roughness 23
5.3 Influence of Model Vibration 30
5.4 Nonuniform Wall Temperature 36
6.0 DISCUSSION OF RESULTS
6.1 Transition on Smooth Cones in Quiet Range 37
6.2 Observed Boundary-Layer Waviness 40
6.3 Experiment with Noise Introduced into Range 41
7.0 CONCLUDING REMARKS 43
REFERENCES 43

ILLUSTRATIONS

Figure

1. Cones Used in Experiments 11
2. Typical Cone Tip Magnified 50X for Inspection Prior to Launch 12
3. Schematic Drawing of Range K Showing Uprange Instrumentation and Launch Tube Location 13
4. Sound Pressure Data Recording System 14
5. Typical Cone Trajectory 17
6. Some Published Data on the Influence of Angle of Attack on Transition Location 18
7. Effect of Angle of Attack on Transition Location, from Ward (Ref. 25) 19
8. Influence of Angle of Attack Compared to Typical Circumferential Variations in Transition Location 20

Figure | Page

9. Kendall's and Ward's Data on the Angle-of-Attack Influence 22
10. Cone with Distributed Roughness 24
11. Cone at Mach 5.1 with Distributed 1700 μin.-rms Roughness 25
12. Cone at Mach 2.2 with Band of 2400 μin.-rms Roughness . 26
13. Effect of Distributed Surface Roughness on Cone at Mach 5.1 27
14. Effect of Localized Roughness at Mach 2.2 27
15. Laser-Front-Lighted Photograph of Cone in Flight 29
16. Apparatus for Studying Vibrational Characteristics of Aluminum and Lexan Cones 31
17. Strain Measurement Apparatus 32
18. Vibrational Response of Aluminum and Lexan Cones . . . 33
19. Smooth-Cone, Quiet-Range Transition Data 39
20. Influence of Elevated Noise Level on Transition Reynolds Number 42

TABLES

1. Experiments on Effect of Angle of Attack on Transition . . . 17
2. Kendall's Experiments on Angle-of-Attack Effect 20
3. Frequency and Amplitude Data 31

NOMENCLATURE 46

1.0 INTRODUCTION

The state of our knowledge of boundary-layer transition has been summarized in notable reviews by Morkovin (Refs. 1 and 2), Mack (Ref. 3), and Mack and Morkovin (Ref. 4). It is a justifiable conclusion, after studying these reviews, that significant, new contributions by experimentalists are necessary and that all possible care must be taken to control and define all factors influencing the transition process in the experimental environment. By far, most previous experimental investigations of transition have been conducted in wind tunnels where it has been generally recognized that coupling between "tunnel" disturbances and flow in the boundary layer under observation almost always made such absolute measurements as local transition Reynolds number, $Re_{\delta,t}$, inapplicable in other environments, even when all of the more obvious dynamic similarity conditions were matched.

Conventional wisdom has led to frequent assumptions that $Re_{\delta,t}$ determined for a model in a wind tunnel must be less than would be found in full-scale free flight where flow disturbances presumably are minimal, but even that has not always been true. Neither does it seem justifiable to condemn all wind tunnel data, as some have done. When the dominant factor influencing transition has been controlled (e.g., roughness, bluntness, sweep, or angle of attack) and results are presented so as to suppress the uncertainty attaching to absolute Reynolds number of transition, useful results may be claimed.

The free-flight range is an experimental facility not widely exploited for boundary-layer transition studies, though much used for wake transition observations. This situation is understandable on grounds of convenience and availability, but some rather important information may be obtained from range experiments. The quiet atmosphere of the aeroballistic range appears to offer an opportunity for study of boundary-layer transition free of the complex influences of stream turbulence and noise which are known to be present in varying degrees in wind tunnels. However, there are some special features of aeroballistic experimentation which raise questions, and it is appropriate that they be reviewed in the context of their influence on boundary-layer transition. The ones discussed in this report are:

1. finite angles of attack and oscillatory motion,
2. surface roughness under conditions of cold walls and large unit Reynolds number,

3. vibration of the model resulting from launch acceleration, and
4. nonuniform surface temperature owing to aerodynamic heating.

The investigation reported in Ref. 5 was conducted to answer the previously unresolved question whether the local Reynolds number of transition, $Re_{\delta,t}$, would vary as local unit Reynolds number, $(U/\nu)_\delta$, varied under aeroballistic range conditions. Such a variation, commonly called a unit Reynolds number effect, was indeed found. Under the conditions existing, it was seen that $Re_{t,\delta} \alpha (U/\nu)_\delta^{0.6}$. This discussion takes Ref. 5 as a point of departure and extends the scope to include a second Mach number, a broader range of unit Reynolds numbers, and study of the above-listed "range-peculiar" factors at both Mach numbers.

The two Mach numbers were selected on the basis of stability theory (cf. Ref. 3) which suggests that different modes of boundary-layer instability are dominant at the two local Mach numbers, M_δ, which were approximately 2.1 and 4.3, respectively. The location of transition was measured on shadowgrams of 4- and 10-deg, semiangle nominally sharp cones at free-stream Mach numbers, M_∞, near 2.2 and 5.1. The range atmosphere was quiescent and free of dust, temperature spottiness, and noise at the model during observation.

2.0 BACKGROUND INVESTIGATIONS

The background of the unit Reynolds number effect found in experiments was traced briefly by Potter in Ref. 5. Morkovin has since presented a general discussion in his review report (Ref. 1). It has been stated several times (cf. Ref. 6) that $(U^2/\nu)_\delta$ may be the more directly relevant parameter, but the unit Reynolds number is the most often used term. In Morkovin's review (Ref. 1), he asserts that the "unit Reynolds number effect" does not represent one effect but a complex superposition of many functional relationships. Thus, he properly cautions against expecting any regular dependence of $Re_{\delta,t}$ on $(U/\nu)_\delta$ under all circumstances. His complete discussion may be read with profit by anyone interested in this subject.

It is well known that U^2/ν appears as a parameter in boundary-layer stability theory, cf. Ref. 3. One may immediately object that

instability and transition are not the same, which is quite true, but the potential value of stability theory as a guide to understanding transition needs no defense. A familiar result from stability calculations following the early work of Tollmien and Schlichting is sketched below. Different flow conditions and different techniques of solution produce different stability boundaries, but the qualitative results are similar to this sketch.

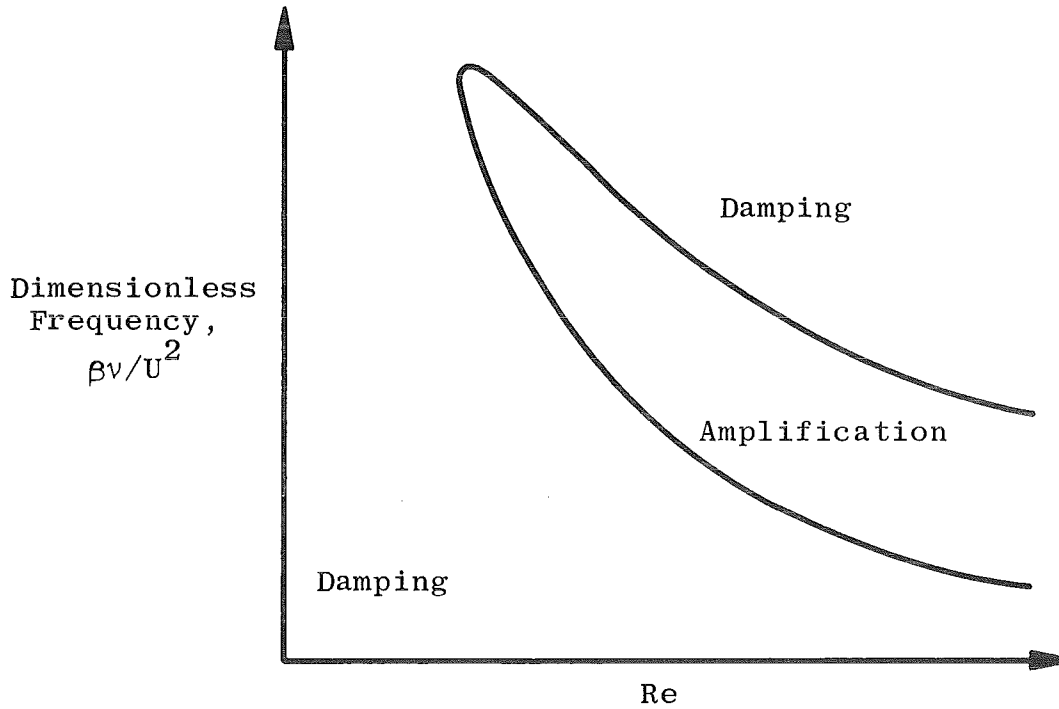

Reynolds Number Based on Boundary-Layer Thickness

Reshotko (Ref. 6) has discussed boundary-layer stability theory with the object of clarifying the roles of $(U^2/\nu)_\delta$ and $(U/\nu)_\delta$. Following Reshotko, consider that the unsteady, compressible-fluid continuity, momentum, and energy equations describe the transition process as well as the other flow regimes. Further assume that all geometric and model surface conditions are essentially constant and are reflected through their contribution to the boundary-layer disturbance spectrum. Then it follows that a Reynolds number characterizing boundary-layer stability may be expressed as

$$Re = f_1(M_\delta,\ T_w/T_\delta,\ \beta\nu_\delta/U_\delta^2,\ \theta)$$

or

$$Re = f_2(M_\delta,\ T_w/T_\delta,\ U_\delta\lambda/\nu_\delta\ c_r,\ \theta)$$

where M_δ is the local Mach number, T_w/T_δ is the ratio of cone wall temperature to local edge-of-boundary-layer temperature, c_r is the phase velocity of disturbance, θ is the characteristic orientation of disturbance spectrum, λ is the characteristic wavelength of disturbance spectrum, and where the dimensionless frequency, $\beta\nu_\delta/U_\delta^2$, is proportional to the dimensionless wavelength, $U_\delta\lambda/\nu_\delta c_r$. If M_δ, T_w/T_δ, and θ are essentially constant, it may be predicted on this basis that the transition Reynolds number may correlate as either

$$Re_{\delta,t} = f_3(\beta\nu_\delta/U_\delta^2)$$

or

$$Re_{\delta,t} = f_4(U_\delta\lambda/\nu_\delta\ c_r)$$

The dimensionless phase velocity, c_r, is a slowly varying quantity at higher Mach numbers.

Although it may not be certain that the unit Reynolds number is the dominant variable, the numerous examples of good correlation of $Re_{\delta,t}$ with U_δ/ν_δ suggest that wavelength may be an important aspect of the disturbance leading to transition. It is possible that both U_δ/ν_δ and U_δ^2/ν_δ enter into the process of transition and that the relations would be clearer if laboratory facilities made it easier to vary U_δ for otherwise fixed conditions. Almost all experiments in which U_δ/ν_δ or U_δ^2/ν_δ are varied at constant Mach number actually involve the variation of ν_δ alone.

Recently, in somewhat limited wind tunnel experiments, Ross (Ref. 7) investigated this question and showed that $(U/\nu)_\delta$ seemed to be more significant than $(U^2/\nu)_\delta$. He produced a variation of $(U/\nu)_\delta$ by changing total temperature at $M_\infty = 4$, and the result was found to be $Re_{\delta,t}$ $\alpha(U/\nu)_\delta^{0.65}$. In the light of the knowledge of tunnel noise influences, see for example Refs, 8 and 9, agreement of the exponent of 0.65 with that found in Ref. 5 may be coincidental. Generally, though by no means always, the exponent has been nearer 0.4 in wind tunnels where $(U/\nu)_\delta$ was varied by changing pressure at constant Mach number.

The correlation of transition Reynolds number with unit Reynolds number in supersonic and hypersonic wind tunnels has been shown to be predictable on grounds of noise pressure fluctuations radiated onto models from turbulent tunnel nozzle boundary layers. Laufer (Ref. 8) demonstrated the influence of unit Reynolds number on sound pressure measurements and achieved an order of ten reduction in $\tilde{p}/p_\infty$ (fluctuating sound pressure amplitude/free-stream pressure) ratio by dropping unit Reynolds number to a level which resulted in laminar nozzle wall boundary layers. Subsequently, Pate and Schueler (Ref. 9) constructed an empirical correlation for $3 \leq M_\infty \leq 8$ using tunnel wall boundary-layer parameters to represent the noise production and the resulting influence on transition on a model exposed to that noise. However, there would seem to be no relationship between those results and the present free-flight range experiments which are believed free of wall influence. At least, none has been suggested yet, and the proposition credited to Morkovin at the beginning of this section probably is as close to an explanation as now exists.

In this discussion of the possible origins of the unit Reynolds number effect, particularly when searching for it in boundary-layer stability theory, it should be remembered that one is not looking at a completely explored and mapped territory. Until all the details of the process leading first to instability and thence to transition can be described, it would not be suprising if some further revelations lie in store.

New viewpoints on the transition process may lead to understanding of the unit Reynolds number effect, but only speculations can be offered here. For example, the role of streamwise vortices is well known in connection with the transitional process occurring in flows between concentric, rotating cylinders, and flows over concave walls. The basic sources of information on such flows are early papers by G. I. Taylor, L. Prandtl, H. Görtler, and others. A convenient summary may be found in Ref. 10. Subsequent research by Liepmann is reported in Ref. 11. More recently, Persen (Refs. 12 through 15) has studied the appearance of streamwise vortices in various flows, including conical flows, and has suggested that the streamwise vortex system is an intermediate stage between the onset of instability of laminar flow and its final transition to turbulence. He contended that this is the case in all transitions of fluid flows and cited Görtler's comments in Ref. 16 concerning the bridging of the gap between two-dimensional instability and three-dimensional, turbulent flow where, Görtler said, a secondary critical Reynolds number may play a role.

There is a persistent tendency on the part of some investigators to make quantitative comparisons between sets of transition data from different experimental facilities, e.g., between wind tunnels and aeroballistic ranges. Aside from differences in recognized but incompletely evaluated parameters such as cone wall temperature, T_W, and free-stream temperature, T_∞, which may vary widely between tunnel and range at a given Mach number, there are other good reasons to reserve judgement when comparing these types of data. Unless the dominant causes of transition are clear and well controlled, there can be no confidence that the disturbance spectra acting on different boundary layers are equivalent. Typically, this information is seriously inadequate because of the major effort needed to acquire it.

Knowledge of the disturbance spectrum would enhance any experimental data. In their studies wherein free-stream perturbations were related to transition on a sharp flat plate in incompressible flow, Miller and Fejer (Ref. 17) found that

1. The Reynolds number at the beginning of transition was influenced only by the amplitude of the free-stream oscillation.
2. The transition distance, i.e., interval of length from beginning to end, was influenced only by the frequency of the free-stream oscillation.

Laufer and Vrebalovich (Ref. 18), from work in a supersonic wind tunnel, have reported that... "The experiments succeeded in detecting self-excited oscillations in the boundary layer. Generally speaking the basic features of these oscillations are the same as found in the incompressible layer and are in agreement with existing theory. Specifically, the boundary layer acts as a frequency selective amplifier with respect to the disturbances; depending on local Reynolds number, it attenuates certain frequencies and amplifies others, thus causing detectable oscillations in a narrow band width."

Whether disturbances originate in a wind tunnel stream or within the flow field of a body in free flight through quiet air would seem to allow large differences in the amplitudes and frequencies which are imposed on boundary layers. Even in the wind tunnel environment alone, possibly significant variations in acoustic characteristics may be encountered. Fahy and Pretlove (Ref. 19) have observed that duct flows may be likened to antenna waveguides in that dead-band regions or cut-off frequencies may exist. Thus, depending on the set of harmonics peculiar to the duct design, sound waves from one source may be

canceled, refracted, or reinforced by waves generated by other sources. Therefore, it is not surprising that the levels of transition Reynolds numbers for given shapes at seemingly equal conditions sometimes differ by factors of two or more between different wind tunnels or between a wind tunnel and an aeroballistic range. In such circumstances, data on the disturbance spectrum may offer the only way to understand the results.

3.0 MODELS AND RANGE SYSTEMS

Data on models are given in Fig. 1. The 1.75-in.-diam aluminum cones were used for the earlier launches, but the 2.5-in.-diam aluminum cone later became the principal model. All Lexan® cones were of 1.75-in. diameter. Only a few 4-deg semiangle cones were used, all at Mach two and at low unit Reynolds numbers.

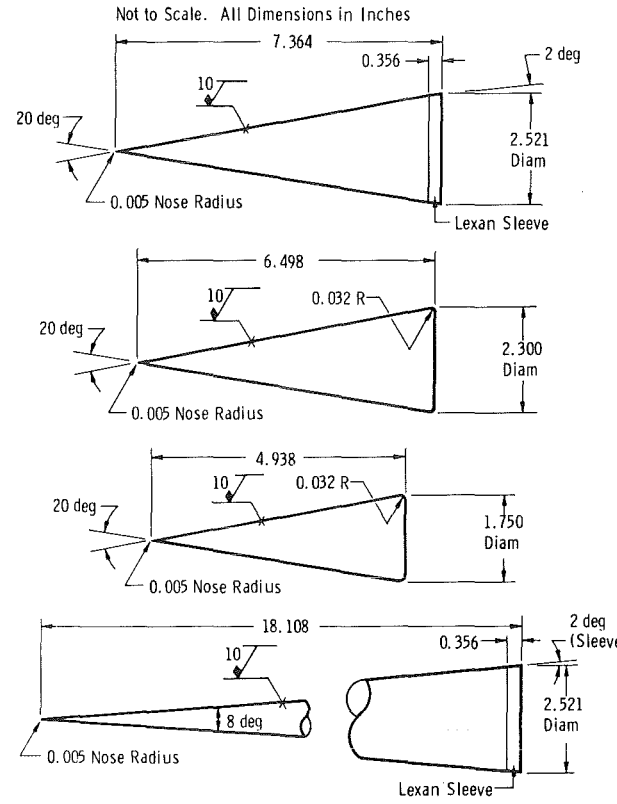

Figure 1. Cones used in experiments (Except as noted on the 2.5-in. cones, all 2.5- or 2.3-in. cone surfaces were aluminum. The 1.75-in. cones were either aluminum or Lexan. Finish of the Lexan cones was approximately 30μin.).

The aluminum models were fabricated from 7075-T6 alloy and were given a surface finish of 10 μin.-rms, or better. (The subject of surface roughness is discussed later.) A nose radius of 0.005 in. was standard on both aluminum and Lexan cones. The latter is polycarbonate resin which was selected because it would give a cone of appreciably different vibrational characteristics for comparison with the aluminum cone. This was wanted for a study of the possible influence of vibration on boundary-layer transition, which is discussed in a later section. At first it was supposed that the Lexan cones would require aluminum tips to prevent ablation, but trial flights in the range proved that an all-Lexan cone surface was feasible under these conditions.

Figure 2 is a typical magnified photograph of the tip of an aluminum cone. It will be noticed that the cone tip in Fig. 2 is closely hemispherical except near the base of the hemisphere where the finishing process symmetrically removed a small amount of material, making the tip somewhat parabolic. As it is confined to a small region, typically about 0.01 in. long, no effect of this type of manufacturing error would be expected.

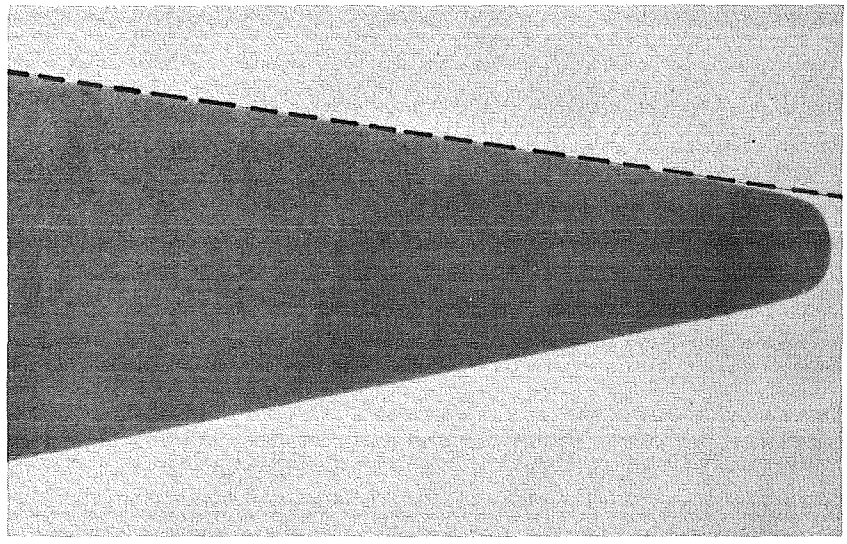

Figure 2. Typical cone tip magnified 50X for inspection prior to launch.

Sabots used with these cones are discussed in the context of their relation to roughening of cone surfaces in a later section. Portions of the sabots in contact with the cones were given finishes of approximately 30 μin.-rms.

The aeroballistic range used for this work was Hyperballistic Range (K) (Fig. 3). This is a 100-ft-long, 6-ft-diam range equipped with six dual-axis shadowgraph systems and a single high-quality schlieren or focused shadowgraph system at the time these studies began. The latter, with an effective exposure duration of 0.15 μsec, was used to obtain the principal photographic data in this investigation. During the later stages of the experiments a second such photographic station was installed. A laser-front-lighted photographic system, with an effective exposure duration of 20 nsec, was used to obtain information on cone surface conditions after launch.

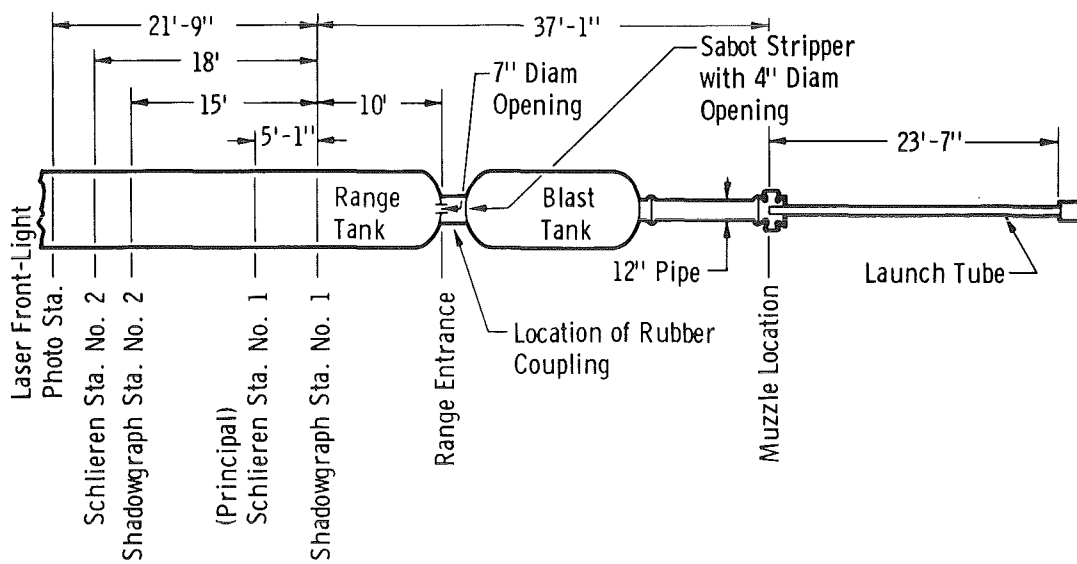

Figure 3. Schematic drawing of Range K showing uprange instrumentation and launch tube location.

A single-stage, 2.5-in.-caliber launcher was used. The muzzle of this gun was located approximately 42 ft from the principal focused shadowgraph station. The cones were launched without spin, and sabot separation was caused by aerodynamic force on the sabot components.

Noise in the range was monitored by small microphones, much as reported in Ref. 5. Except during some brief trial launches with a siren in the range, 0.25-in. Bruel and Kjaer® (B & K) microphones were used. For the trial with a siren, described later, a B & K 0.5-in. model was installed. Figure 4 shows a simplified layout of the microphone data system. Some pertinent characteristics of the complete system for sound pressure measurement follow:

Dynamic Range: 70 to 174 db-rms, referenced to 0.0002 μbar

Limiting Sound Pressure: 185 db

Response: ±3 db from 40 Hz to 40 kHz at pressures and temperatures of this investigation

4.0 RANGE AIR CONDITIONS

During the work reported in Ref. 5, the only measurable disturbances in the range air arose from vibration of the range structure. The dominant cause of this was traced to the impact of the sabot sections on the stripper located in the blast tank between the launcher muzzle and the opening into the range proper. Figure 3 illustrates the structural arrangement during the present launchings. If the sabot impact on the stripper were allowed to transmit disturbances through the steel tank structure at the speed of sound in that material, these disturbances would arrive in the wall near the photographic station well ahead of the cones. Vibrations of the structure are transmitted to the adjacent air, so it is apparent that disturbances would be introduced into the air ahead of the cones unless their speed is sufficient to outrun the structure-to-air noise. This was illustrated in Ref. 5.

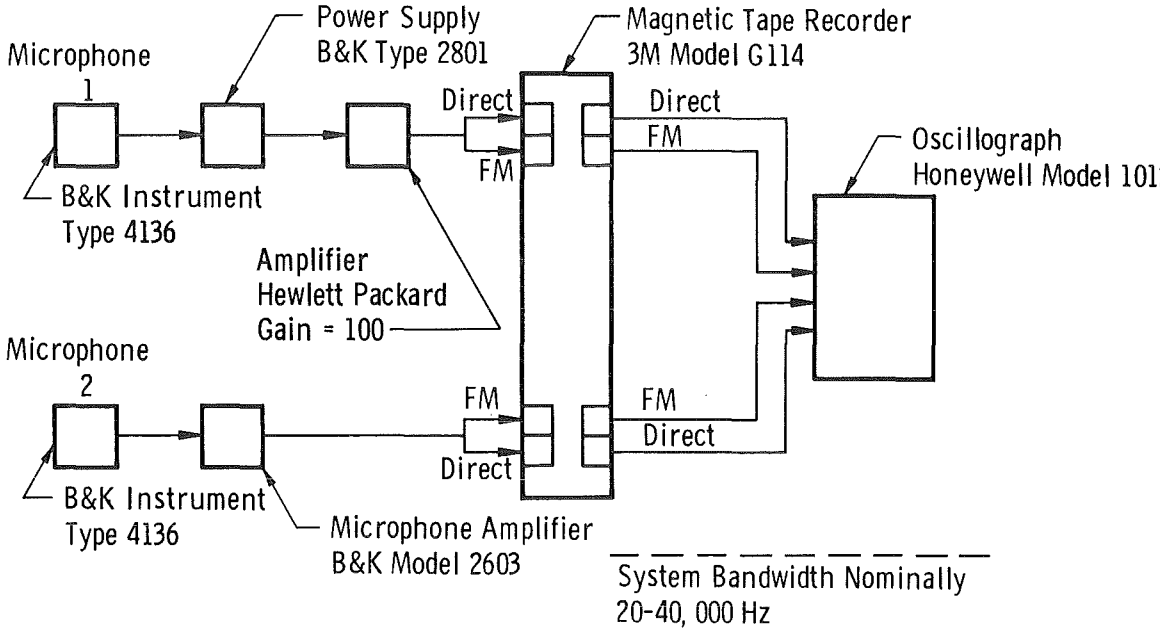

Figure 4. Sound pressure data recording system.

To suppress this noise near its dominant source, a heavy rubber coupling was installed between the blast tank and the range entrance as shown in Fig. 3. This simple step proved highly effective in that no significant sound pressure level was measurable near the centerline of the range at the photographic stations prior to arrival of the cones at either Mach two or five. Based on the characteristics of the microphone system described earlier it is concluded that sound pressure level in the 40-Hz to 40-kHz regime was therefore

$$\tilde{p} \approx 4.7 \times 10^{-4} \text{ mm Hg, rms}$$

Using the lowest value of p_∞, this gives

$$(\tilde{p}/p_\infty)_{max} \approx 2 \times 10^{-6}, \text{ rms}$$

This is several orders of ten lower than the levels measured in supersonic wind tunnels at Mach three, cf. Refs. 8 and 9. However, the earlier discussion of disturbance spectra and the uncertainty about the relative importance of different amplitude-frequency bands should discourage quantitative speculation on the effect of this low-noise environment on transition Reynolds numbers.

Considering that the range air had long settling times between pumping or venting operations and was always near room temperature, there was little likelihood of measurable turbulence or temperature spottiness existing immediately prior to launches. The question of suspended dust was investigated by conducting tests using techniques developed for clean-room monitoring. Repeated tests always showed the number of dirt particles to be less than the level expected in an office area. The data scattered about the curve defining a class 10,000 clean room.

5.0 SOME FEATURES OF AEROBALLISTIC EXPERIMENTATION

This section is devoted to discussion of the aeroballistic conditions that were mentioned in Section 1.0, namely:

1. finite angles of attack and oscillatory motion,
2. surface roughness,
3. vibration of the model resulting from launch acceleration, and
4. nonuniform surface temperature owing to aerodynamic heating.

Although these may be present in wind tunnels too, they are more likely to be factors under aeroballistic range conditions. If free-stream disturbances are negligible in a range and if external disturbances are necessary for instability and transition in a boundary layer, then candidates may be found in the above list.

5.1 INFLUENCE OF ANGLE OF ATTACK

It is rare that a free-flight model maintains zero angle of attack throughout its flight. Under the best conditions, aeroballistic models may have near-zero average total angle and exhibit amplitudes of only one or two degrees. However, the typical range is equipped with only a few schlieren or shadowgraph stations of the high quality needed for photographing boundary-layer transition, and the photographic data on the models launched inevitably will include a random distribution of angles. Note that one must distinguish between the total angle and the angle in the plane of the photograph; they usually will be different. The range pressures in transition work usually are relatively high, which aids in damping the model motions, but the observation station for transition studies on high-speed, sharp-nosed models usually must be located rather near the launcher to obtain data prior to ablation of the model. Thus, finite and variable angles of attack must be expected.

For the experiments discussed herein, Fig. 5 is typical. The angles in two planes are plotted as a function of length along the range, measured from the first to the last of six dual-axis shadowgraph stations. The M and N planes refer to the two orthogonal film planes of the shadowgraph cameras. The principal, parallel-light, single-axis shadowgraph station was located at 5 ft on the length scale given. This typical case is characterized by an average velocity of approximately 5700 ft/sec, a quarter-cycle of motion in roughly 17 ft, and a maximum amplitude somewhat under 2 deg. The wetted length of the conical model upstream of transition in this case was slightly under 5 in. Thus, there was a change in angle of attack of 2 deg in 17 ft of flight or 0.0029 sec, giving a rate of change of 690 deg/sec. In terms of wetted-length-to-transition, the velocity was 13,700 lengths/sec. This enables expressing the oscillatory motion as 690/13,700 = 0.05 deg/wetted length. If one assumes that the change in angle of attack during a time corresponding to flow from stagnation point to transition location is crucial, then this information seems to warrant the tentative assumption that the oscillations of the models, per se, in these experiments were of low enough frequency for that to be ignored as a factor in boundary-layer transition.

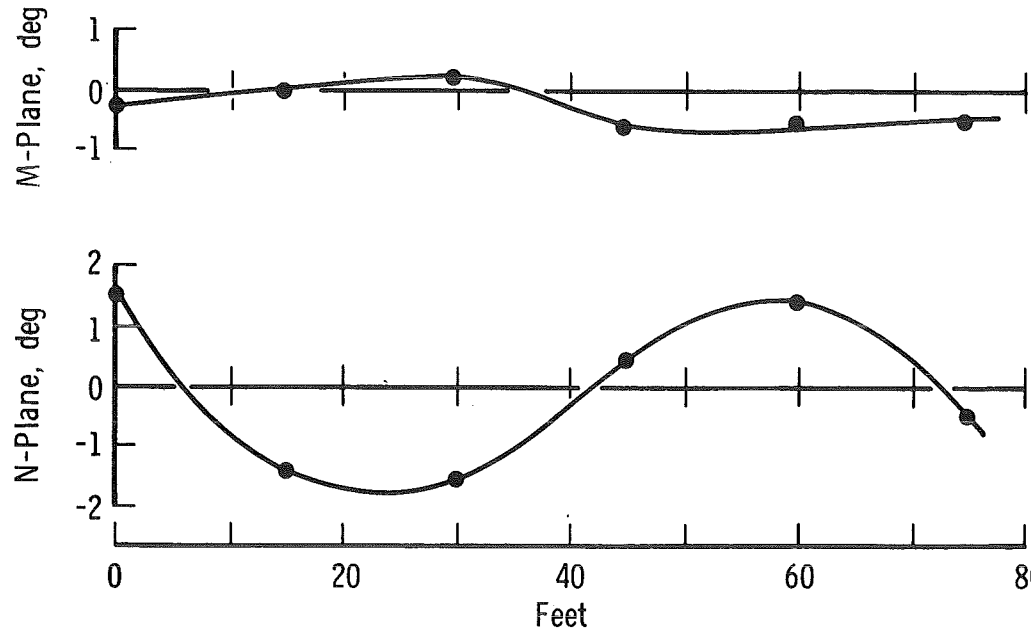

Figure 5. Typical cone trajectory.

There have been several reports on the effects of small angles of attack, α, on transition location on cones. Some of the data are summarized in Fig. 6, and Table 1 gives supplemental information.

Table 1. Experiments on Effect of Angle of Attack on Transition

Ref.	θ_c, deg	M_∞	T_w/T_{aw}	Re_∞ in.$^{-1}$ x 10^{-6}
20	2.87	21.5	~1	1.19
21	8.0	5.5	0.2 - 0.6	0.11 - 0.34
22	10.0	6.9	~0.55	0.38
23	5.0	8.0	~0.4	1.14
24	8.0	10.2	~0.3	0.175
25	10.0	6.0	~0.86	1.10

where θ_c is the cone semiapex-angle and T_{aw} is the adiabatic wall temperature. For comparison, the present conditions are:

10.0	5.1	~0.18	0.76 - 8.1
4 & 10	2.2	~0.50	0.31 - 3.1

The authors of Ref. 21 ignored the possibility of a unit Reynolds number influence in drawing the curve reproduced in Fig. 6, i.e., they compared points for $\alpha = 0$ and $\alpha \neq 0$ which did not correspond to constant U/ν. The curve marked 21a represents the result of an effort to adjust the results of Ref. 21 on the basis of an assumed $Re_t \propto (U/\nu)^{1/2}$ relation. It is shown only to indicate qualitatively how much influence may have existed.

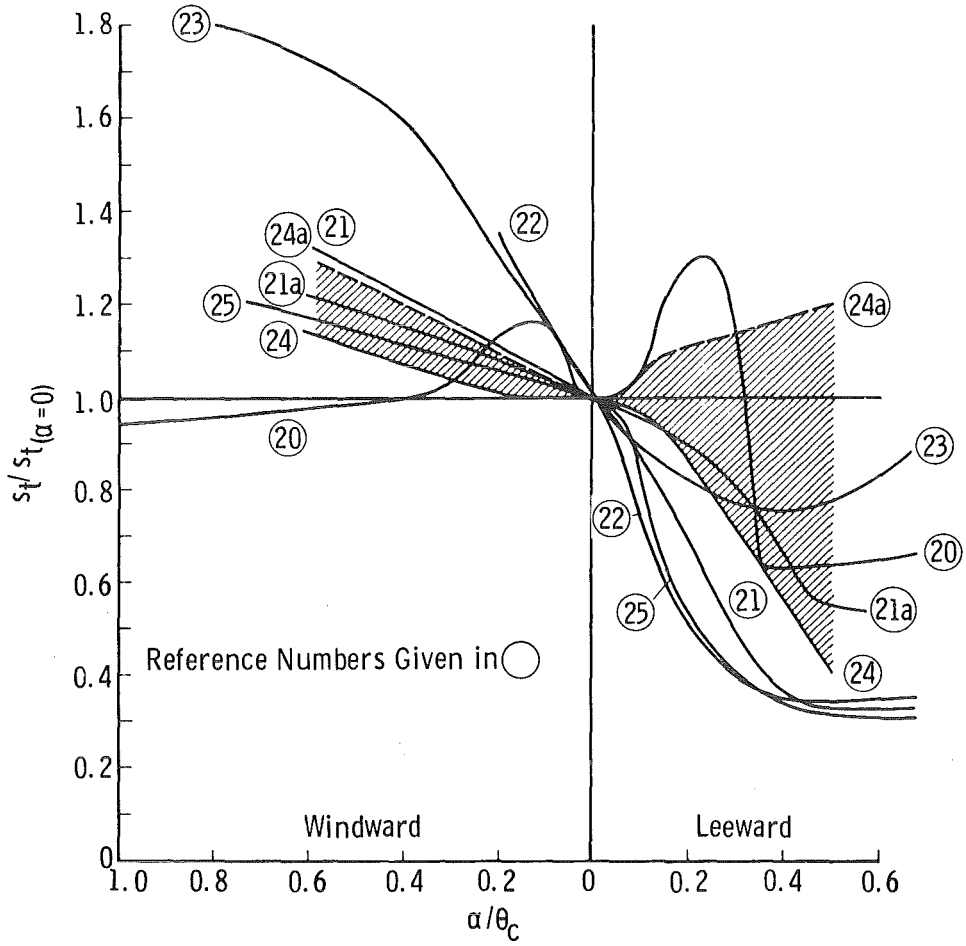

Figure 6. Some published data on the influence of angle of attack on transition location.

The curves marked 24 and 24a represent the extremes of the data of Ref. 24. Curve 24 represents $\phi = 0$ and 180, where ϕ is measured from the windward stagnation line on the cone surface to the meridian in question. As ϕ varied at fixed α, s_t values between curves 24 and 24a were found.

Table 1 shows that most of the conditions represented in Fig. 6 are not directly comparable to the conditions of the present investigation. The roles of Mach number and even cone angle cannot be easily seen, probably partly because of experimental scatter and the influence of additional factors. Some of the referenced material shows evidence that nose bluntness and Reynolds number also are factors to consider in correlating such data. Note that transition location does not vary as would be expected on the basis of changes in local unit Reynolds number when α varies. Apparently, cross-flow effects dominate, i.e., cross-flow and related viscous-fluid phenomena are more important than changes in local "inviscid" flow properties.

Ward's results (Ref. 25) are of interest because the experimental conditions, M_δ, θ_c, and $(U/\nu)_\delta$, were close to the present Mach five case. A modification has been made to Ward's result which consists of refairing his curves between 0 and 1 deg leeward, as shown in Fig. 7. The result is not in conflict with Ward's data, and it seems to agree better with the present range data (if such a fine point is justified here).

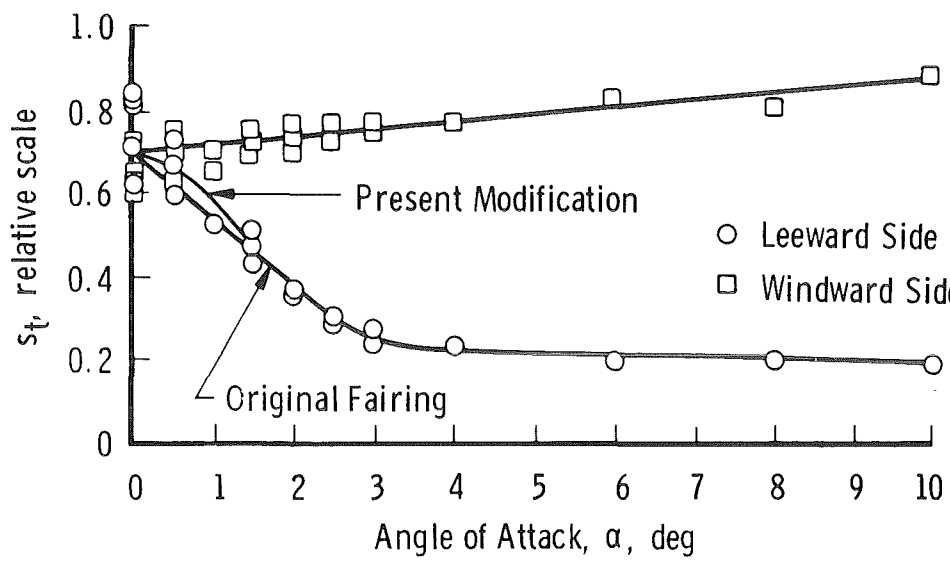

Figure 7. Effect of angle of attack on transition location, from Ward (Ref. 25).

Under the auspices of a NASA Transition Study Group chaired by Eli Reshotko, the writer had a series of contacts with J. M. Kendall, Jr. of the Jet Propulsion Laboratory in Pasadena, California. Dr. Kendall agreed to conduct experiments in the NASA/CIT Jet Propulsion Laboratory 20-in. supersonic wind tunnel with the objective of determining the angle-of-attack influence on transition under conditions as close as

practicable to those of the present free flights. Access to his results was very helpful during the analysis of the free-flight data. The conditions are shown in Table 2.

Table 2. Kendall's Experiments on Angle-of-Attack Effect

θ_c, deg	M_∞	M_δ	T_w/T_{aw}	Re_∞ in.$^{-1}$ x 10^{-5}
4.0	2.2	2.15	1	4.5 maximum
10.0	2.2 - 4.8	2.03 - 4.10	1	4.5 maximum

One interesting result of the wind tunnel experiments is shown in Fig. 8, which was provided in advance of publication by Dr. Kendall.

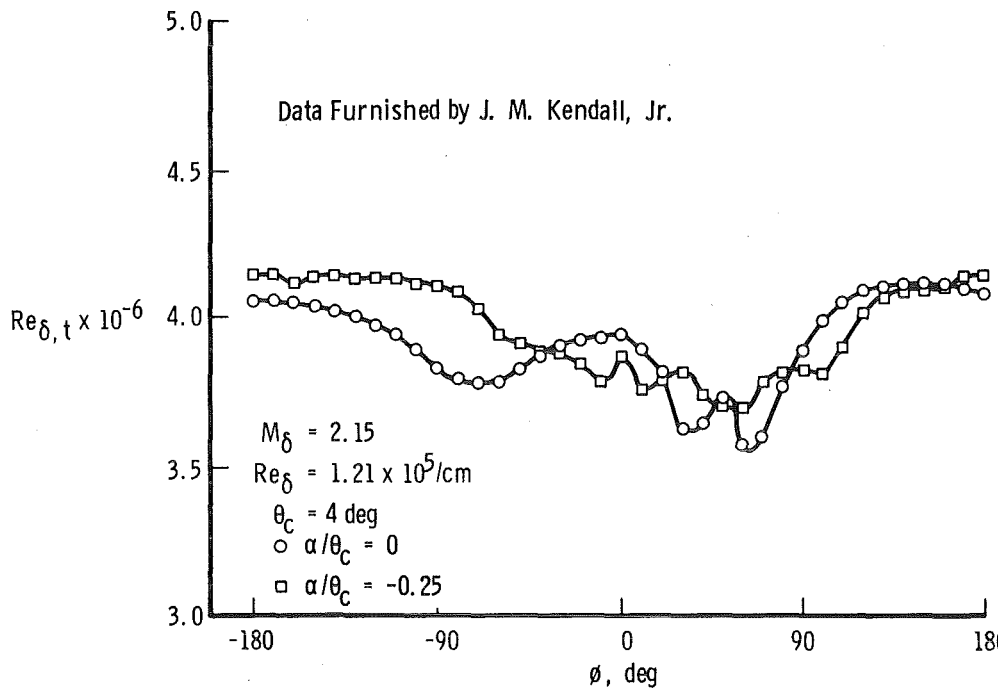

Figure 8. Influence of angle of attack compared to typical circumferential variations in transition location.

It is revealing to see that the natural circumferential variation of transition location at α = 0 was at least as uneven as the distribution at α = 1 deg or α/θ_c = 0.25. The spread between the two curves in Fig. 8 is less than the scatter of the aeroballistic range data to be discussed later. Therefore, it is concluded that, for $\alpha/\theta_c \leq 0.25$ at least, there

is no need to account precisely for meridian angle or circumferential variations in the range data when $\alpha_p \neq \alpha$ (where α_p is the angle of attack in the plane of the photograph). On the windward sides of cones, where the influence of angle of attack is small, this would suggest that meridian angle is unimportant for α/θ_c appreciably larger than 0.25. The writer also has observed that, typically, transition location on a cone at small angle of attack does not vary significantly or systematically with meridian angle up to $\phi = \pm 110$ deg for $\alpha/\theta_c \lesssim 0.5$. That is, the data spread with roll at $\alpha = 0$ is as great as the change in $Re_{\delta,t}$ with α up to $\alpha/\theta_c \approx 0.5$, cf. Refs. 24 and 27. Note that, for small values of α and α_p,

$$\cos \phi \approx \pm \alpha_p/\alpha$$

Thus, for example, the edges of the cone profile seen in a photograph correspond to

$$\phi = 0 \text{ or } 180 \text{ deg when } \alpha_p = \alpha$$

and

$$\phi = 90 \text{ deg when } \alpha_p = 0 \text{ but } \alpha \neq 0$$

In Fig. 9, Kendall's results for the influence of angle of attack are compared with Ward's, and remarkably good agreement is apparent. Of course, such a direct comparison is not justified in view of the Mach and Reynolds number differences, but the agreement is pointed out because it justifies using only one α-correction curve for all of the present conditions if, say,

$$\alpha/\theta_c \text{ (leeward)} < 0.25$$

Nevertheless, a problem remains with the lee data for $\alpha_p \neq \alpha$, even when the above limitation is imposed. At $\alpha/\theta_c = 0.25$ in Fig. 9, the correction factor for lee-side readings is 0.48, at $\phi = 180$ deg and $\alpha_p = \alpha$. But the author's observation is that a correction factor near 1 is justified if $\phi \lesssim 110$ deg and $\alpha_p \neq \alpha$, where ϕ is the meridian angle representing the edge of the silhouette of the cone as seen in the focused shadowgram.

Considering the inherent scatter of transition location, particularly when single-shot, high-speed photographic data are used, and the uncertainties in angle-of-attack correction, it was decided to adopt the following criteria for acceptance of data in the present experiments:

1. Use windward data for $\alpha/\theta_c \leq 0.6$. Few exceeded 0.3.

Sym	θ_c, deg	M_δ	$(U/\nu)_\delta$ in.$^{-1}$	Ref.
○	4	2.15	4.5×10^5	26
□	10	2.03	4.5×10^5	26
— — —	10	4.99	11×10^5	25

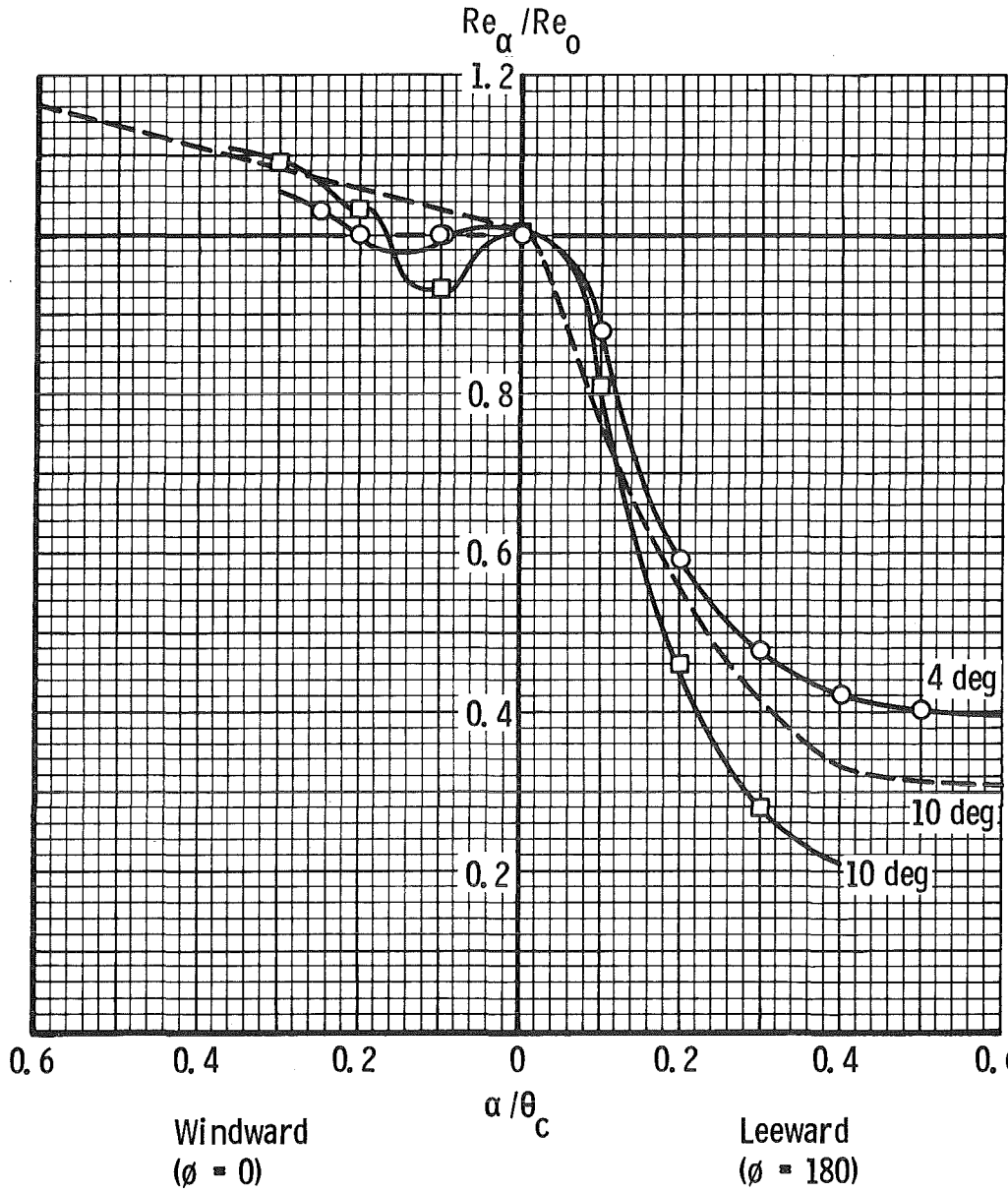

Figure 9. Kendall's and Ward's data on the angle-of-attack influence.

2. Use leeward data for $\alpha/\theta_c \leq 0.25$ but only when corresponding windward data are available for support.

3. Disregard the difference between α and α_p, under the restrictions of (1) and (2), when dealing with $\phi \leq 110$ deg.

4. Let the factor of Fig. 9 for lee readings vary linearly from the value given in Fig. 9 for $\phi = \pm 180$ deg to a value of 1.0 as ϕ goes from 180 to 110 deg. This is consistent with the data in Refs. 24 and 27 where, within the basic scatter of the data for fixed α, there is roughly a linear variation of $Re_{\delta,t}$ with ϕ in the region of concern.

5. Base the correction of all data on Ward's curve on Fig. 9.

6. Disregard the effect of small angles of attack on local M and Re.

Attention is directed to the more complete method for analyzing angle-of-attack effect on transition presented by Mateer (Ref. 27). That degree of effort to refine the present data was not deemed necessary in view of the other influences on the scatter.

5.2 INFLUENCE OF SURFACE ROUGHNESS

Because of the typically higher local unit Reynolds number, cold walls ($T_w < T_{aw}$) and consequently thin boundary layers, it has been suggested that transition data from aeroballistic ranges may be affected by surface roughness. Although a method exists for predicting the influence of standard, raised roughness on transition (Ref. 28), it was thought best to conduct some experiments under actual aeroballistic range conditions. This was done at Mach numbers of five and two.

In the Mach five phase, which was done first, cones otherwise identical to the 1.75-in. models in Fig. 1 were deliberately roughened, as sketched in Fig. 10. Considering that circumferential machine tool marks, or grooves, seemed to be the most general form of roughness encountered on nominally smooth conical bodies, the desired roughness was created simply by changing cutting tool speed. That produced varying degrees of circumferential roughness which was measured in the usual manner with a profilometer. The shortcomings of such devices for surface roughness measurements are well known. Mainly, the objections are the possible scratching of the surface by the stylus and the inordinately large radius of the profilometer stylus (500 μin.) compared to the smaller dimensions of the roughness. A typical, well-finished

cone surface registered less than 10 μin.-rms, but one must assume that the profilometer stylus could not penetrate to the bottom of surface defects with transverse widths less than stylus diameter, cf. Ref. 29. Whether such types of roughness are of any importance in a given case is another subject to consider. In view of the data to be shown later, it is probable that defects of this scale did not matter in the experiments discussed herein.

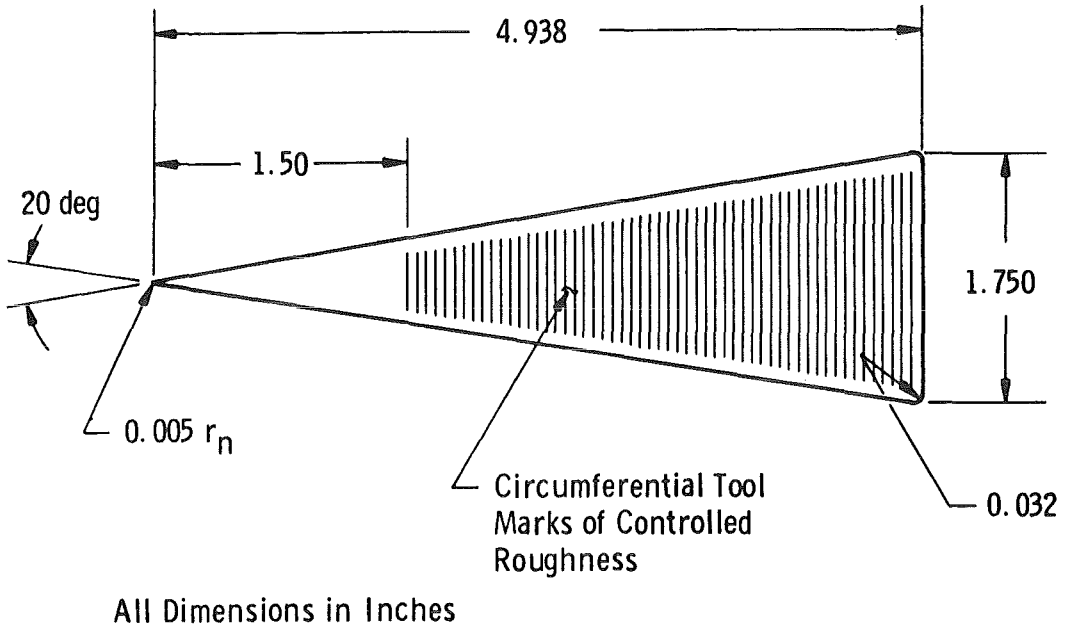

Figure 10. Cone with distributed roughness.

When the time arrived for the experiments on roughness effect threshold at Mach two it was decided to use a narrow band of grooved or screw-thread roughness rather than the widely distributed roughness sketched in Fig. 10. In addition to yielding data on a different type of roughness, the changed procedure made "reading" the shadowgrams a little easier. Only 2.5-in.-diam cones were used for the Mach two studies.

Six circumferential V-grooves (screw-threads) were machined in the aluminum 2.5-in.-diam cones beginning 1.5 in. from the apex (cf. Fig. 10). Thus, the band extended only about 1/10 in. along the cone. Design of the screw-thread was selected so that profilometer readings on the distributed roughness described previously and on the six rows

of threads were consistent. In both cases, the actual dimension from the bottom of a groove to the top was approximately four times the quoted profilometer rms roughness reading. The tops of the grooves lay on the finished surface of the smooth cone, i.e., the threads were cut as shown below:

Figure 11 represents a cone in flight at Mach five with distributed roughness, and Fig. 12 shows a cone at Mach two with a narrow band of roughness. Figure 13 gives the results for the Mach five distributed roughness, while Fig. 14 presents similar results for the Mach two localized roughness. The significant point to be made here is that no effect on transition was discerned until levels of roughness were extended well above those measured by the same technique on nominally smooth cones (~10 μin.-rms) which were used for the main body of this research. Even though the critical roughness seems safely higher than any to be expected on the "smooth" cones used in this study, further experiments were conducted because of some markings seen on free-flight cones.

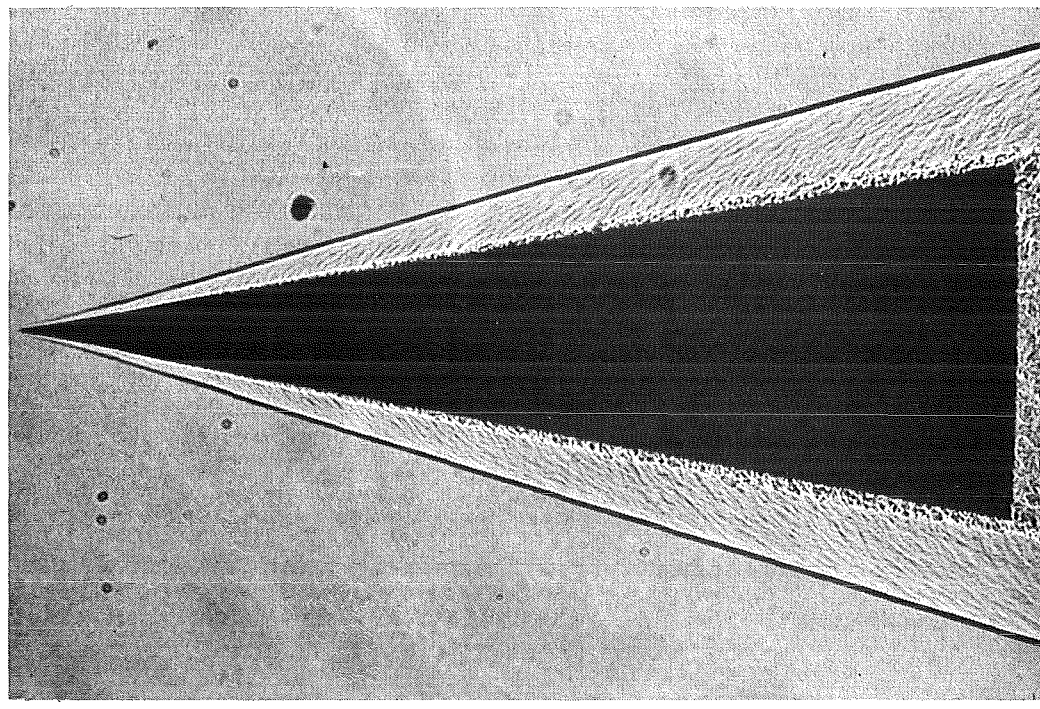

Figure 11. Cone at Mach 5.1 with distributed 1700 μin.-rms roughness.

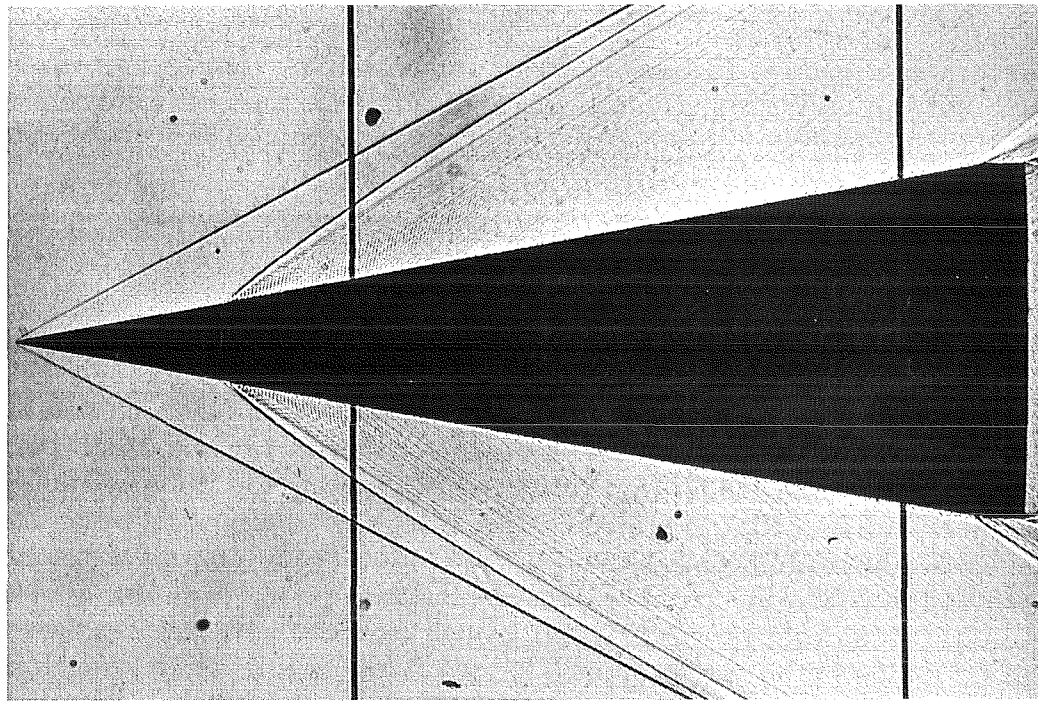

Figure 12. Cone at Mach 2.2 with band of 2400 μin.-rms roughness.

It must be remembered that it is surface condition in flight at the observation station which really matters. Thus, laser-front-lighted photography of the cones in flight has been used as a means for identifying any cones with visible defects such as roughened, bent, or ablated surfaces. The technique, as applied to high-speed, free-flight ablation research, has been described by Dugger, Enis, and Hill (Ref. 30).

Two basic types of sabots have been used in this work. In the prior work (Ref. 5) and part of the recent investigation, closed-base sabots were used. For all of the 2.3- and 2.5-in. aluminum cones used later, open-based sabots were used. The following sketch shows the principal features of these designs, all of which were used with a gun of 2.5-in. caliber.

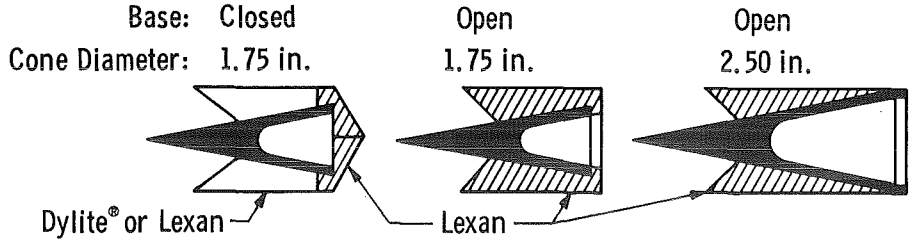

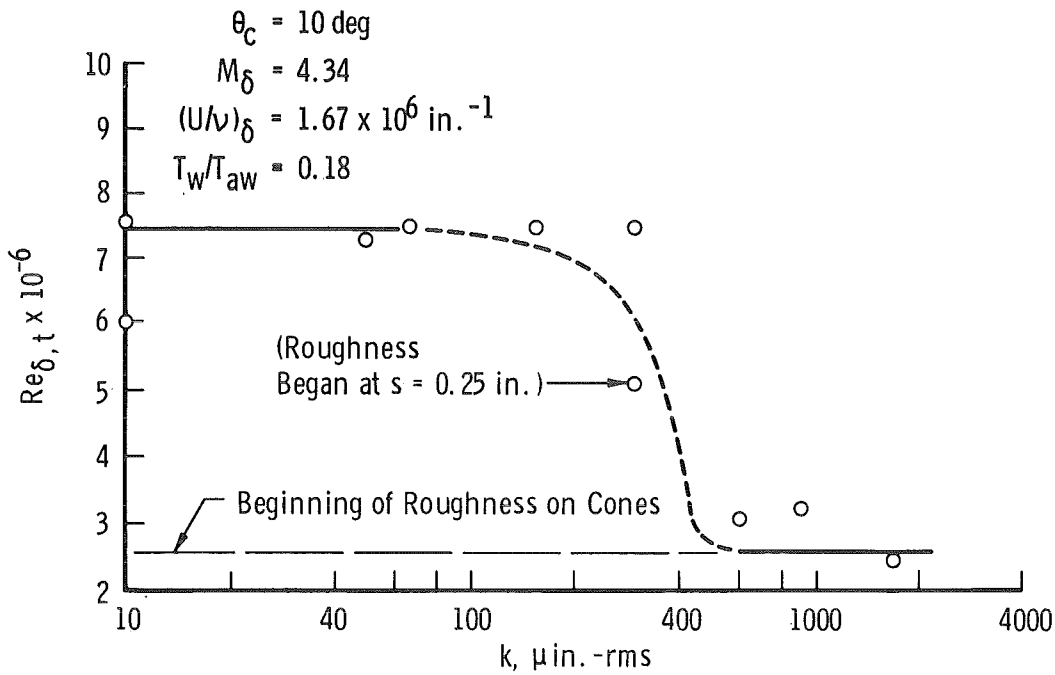

Figure 13. Effect of distributed surface roughness on cone at Mach 5.1.

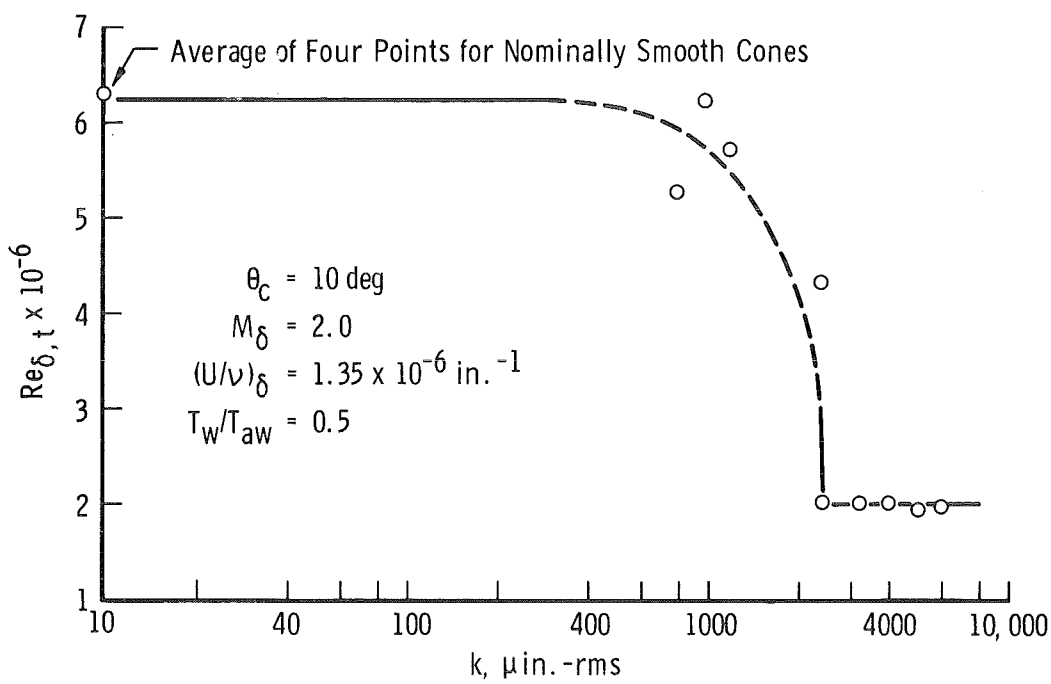

Figure 14. Effect of localized roughness at Mach 2.2.

One sees that under the pressure of the gun gas the sabot pushes on the cone if the sabot is a closed-base design. Masses and base areas of the open-based sabot for sub-caliber cones are adjusted so that the cone pushes on the sabot. For full-caliber cones and open-based sabots, it is obvious that the cone pushes on the sabot during launch. The point of this discussion is that launch loads are great and the cone wetted surface may be roughened if there is sufficient interaction as the cone presses into the open-based sabot. Open-based sabots were developed because there is evidence that they lead to less disturbed launches and lower angles of attack after the sabot separates from the cone.

Cones in these experiments were made from either 7075-T6 aluminum alloy or Lexan. The latter was used for the cones in the study of vibration discussed in the following section. The open-based sabots for the aluminum cones and the closed-base sabots for the Lexan cones were of Lexan, whereas the major portion of the closed-base sabots interacting with the surfaces of the other aluminum cones was Dylite. The latter is a soft plastic much used for inexpensive ice chests and packaging. During the experiments of Ref. 5, closed-base sabots made of Lexan were used.

Aside from a few cases of cone damage in launch, e.g., bent noses on the 4-deg cones, the most important finding in the laser-front-lighted photographs was discolored areas on the cone surfaces where cone and sabot were in contact. An example is Fig. 15. Such markings were seen at various times for all types of sabots used.

Laser-front-lighted photography of static aluminum cones subjected to simulated launch loadings in open-based sabots revealed that the discolored area of Fig. 15 could be approximated with roughnesses measuring only 15 μin.-rms. Early in this investigation, it was also found that the inner surfaces of the Lexan sabots contacting the cones were characterized by profilometer readings of the order of 100 μin.-rms. Thereafter, it was decided to require inner Lexan sabot surfaces to be finished to the order of 30 μin.-rms, which is deemed about the best to be expected on a routine basis from ordinary lathe work on Lexan. Then, it seems a safe assumption that any scuffing or embossing caused by the cone pressing against the sabot would be less than 30 μin.-rms, particularly since the aluminum is the stronger of the two materials. The Dylite foam is so soft, in comparison to aluminum, that any interaction under launch loading should not appreciably roughen the aluminum cones. In addition, the closed-base sabot causes the base of the cone to carry the load, rather than the cone wetted surface, and

this lessens the likelihood of surface embossing. More importantly, no difference in transition data was detected in comparisons between "early" and "later" sabot usage. That is, of course, consistent with the results in Figs. 13 and 14 if the roughness caused by the sabot is no more than 0 (100 μin.).

The zig-zag or saw-tooth pattern of the discoloration on the free-flight cone in Fig. 15 deserves explanation. The sabot quarters have serrated surfaces where they fit together. This is to form a seal against leakage of gun gases and to prevent slippage of the sabot quarters relative to one another. It was clear that the pattern seen in Fig. 15 fitted the sabot serrations, but it was not known if the roughness represented by this pattern was high enough to be important. Presumably the "printing" was caused by hot powder chamber gas leaking through the seals from the base of the sabot, possibly enhanced by contaminants produced as the sabot was heated by the propelling gas and by friction along the gun barrel.

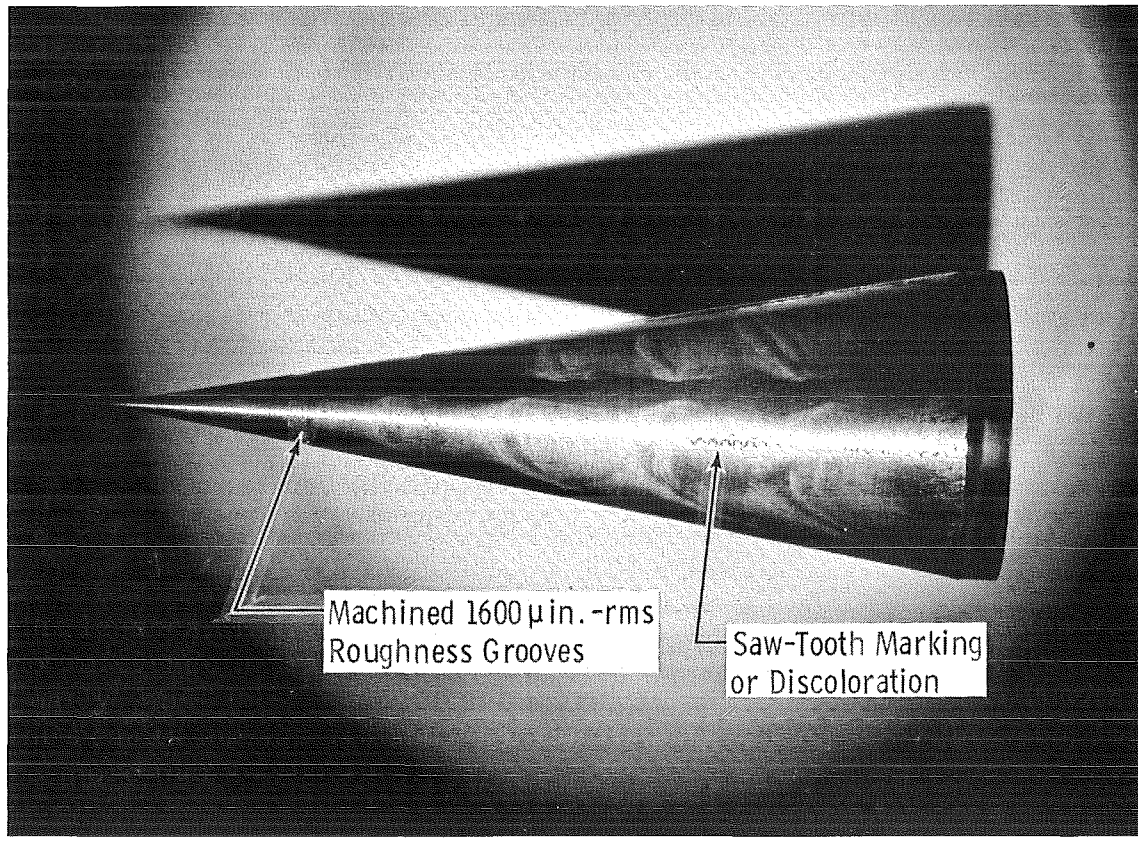

Figure 15. Laser-front-lighted photograph of cone in flight.

To resolve the question raised by the leakage-related, printed pattern described above, a technique of wrapping the cones with a thin, single-layer sheet of Mylar® was adopted. The Mylar was wrapped around the cones so that all four longitudinal sabot joints were fully covered by the protective sheet. During launch, after exit from the gun barrel, the Mylar sheet was quickly swept aside and fell to the floor. This left the cones unmarked by the sabot serrations. The technique was successful on every launch of 2.5-in.-diam, 10-deg cones in open-base sabots. The latter was the only type of sabot used during this phase of the investigation. It was not successful when 4-deg cones were used. Evidence picked up off the blast tank floor showed that the Mylar sheet was cut or burned through in a saw-tooth pattern where it fitted against the serrated sabot joints.

Considering that no difference in transition data was found in comparing data for Mylar-wrapped and unprotected 10-deg cones, it seems safe to conclude that the printed, longitudinal, saw-tooth patterns did not systematically influence the results. The Mylar-wrapped cones will be identified when transition data are discussed later in Section 6.0.

In view of Figs. 13 and 14, and the other results described, it is concluded that surface roughness has not significantly affected the data presented in Ref. 5 or any of the later data reported herein. And further, roughness can be regarded as a negligible factor in relation to the data for any of the so-called smooth cones under conditions where the method of Ref. 28 predicts no influence.

5.3 INFLUENCE OF MODEL VIBRATION

The possible influence of model vibration was examined by comparing transition results obtained from launching cones of two materials under otherwise similar conditions. The materials were chosen on the basis of their being compatible with the rigors of range operations while having appreciably different vibrational characteristics. If one made a significant change in transition location by this variation in cone vibrational behavior, it at least would indicate the need for more careful study. Seeing no change does not prove that cone vibration is not a factor, but the experiment seemed worthwhile.

All the previous work, as well as the current extension, involved aluminum cones. The only readily usable material offering significantly

different vibrational characteristics appeared to be Lexan. Table 3 shows relevant data on the two materials.

Table 3. Frequency and Amplitude Data

Material	W	Y
Aluminum 7075-T6	1	1
Lexan	0.28	3.3

$W = (E/\rho)^{1/2}/(E/\rho)^{1/2}_{aluminum}$

= frequency ratio

$Y = (\sigma_y/E)/(\sigma_y/E)_{aluminum}$

= amplitude ratio

E = Young's modulus of elasticity

ρ = material density

σ_y = yield strength in tension

Laboratory experiments have essentially confirmed the computed frequency ratio in Table 3. These experiments took two forms. First, the 1.75-in.-diam aluminum and Lexan cones were simulated by models in the manner shown in Fig. 16.

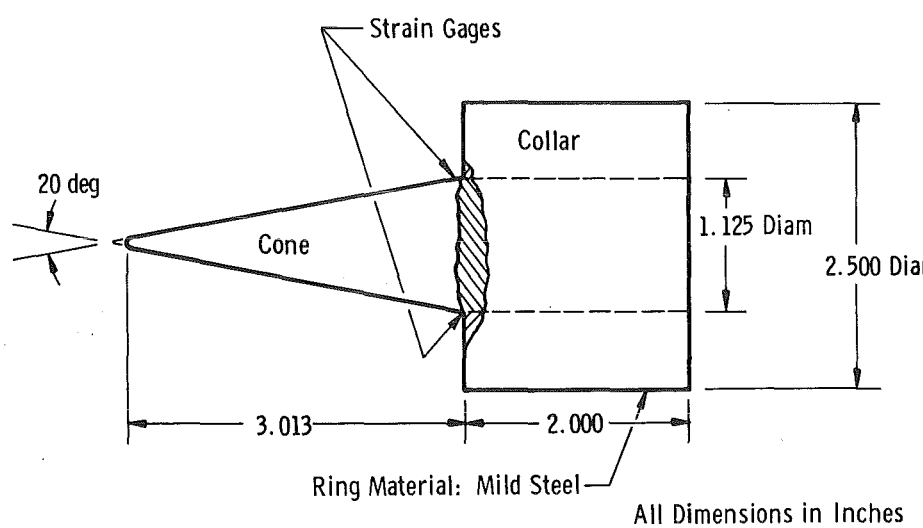

Figure 16. Apparatus for studying vibrational characteristics of aluminum and Lexan cones.

The assumption was made that the cone tip in free flight would tend to vibrate as if the cone were fixed at its center of gravity, as in Fig. 16. The length of 3.013 in. that the cone extends from the support collar also was the distance from the tip to the center of gravity of the 1.75-in. free-flight cone. Strain gages were attached to the base of the cone and wired to measure bending stress. The collar was suspended from wires and struck with a hammer or ball bearing to induce vibration in the cone.

Bending strain at the base of the cone simulating the range models was measured with two strain gages which formed adjacent arms of a four-equal-arm bridge circuit as shown in Fig. 17. The bridge was powered from a 6-v battery. Strain, represented by the bridge output, was amplified using a differential-type d-c amplifier and was recorded using a preamplifier and an oscilloscope. A 3-v common mode voltage was provided by a resistance voltage divider so that zero voltage would appear at the amplifier inputs with the bridge balanced. The oscilloscope was triggered internally from gage output. The strain recording system was calibrated by unbalancing the bridge circuit with fixed resistors paralleled with one arm of the resistance bridge.

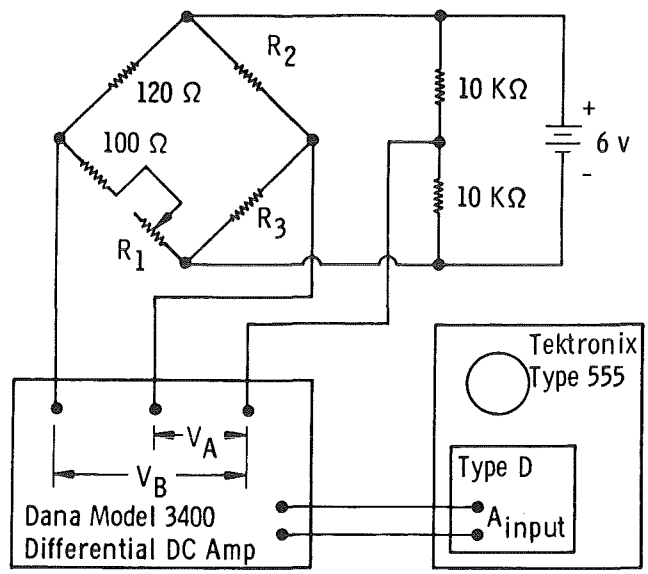

Notes: (1) R_1 is a 25 Ω, carbon potentiometer.
(2) R_2 and R_3 are SR4 Type FAE-03N-1256 strain gages.
(3) Bridge output is $V_A - V_B$.

Figure 17. Strain measurement apparatus.

Oscilloscope traces as shown in Fig. 18 were obtained when the cones were struck with a large ball bearing. The lower frequency and greater amplitude of the Lexan cone is obvious. It should be noted that the so-called Lexan cone is not truly representative of a cone made only from Lexan; for aerodynamic stability it was necessary to insert internal metal ballast in the fore part of the cone. This affected the vibrational characteristics, and it is the ballasted cone which is represented in Fig. 18. Apparently, the ballast acted as a damper because it reduced the frequency.

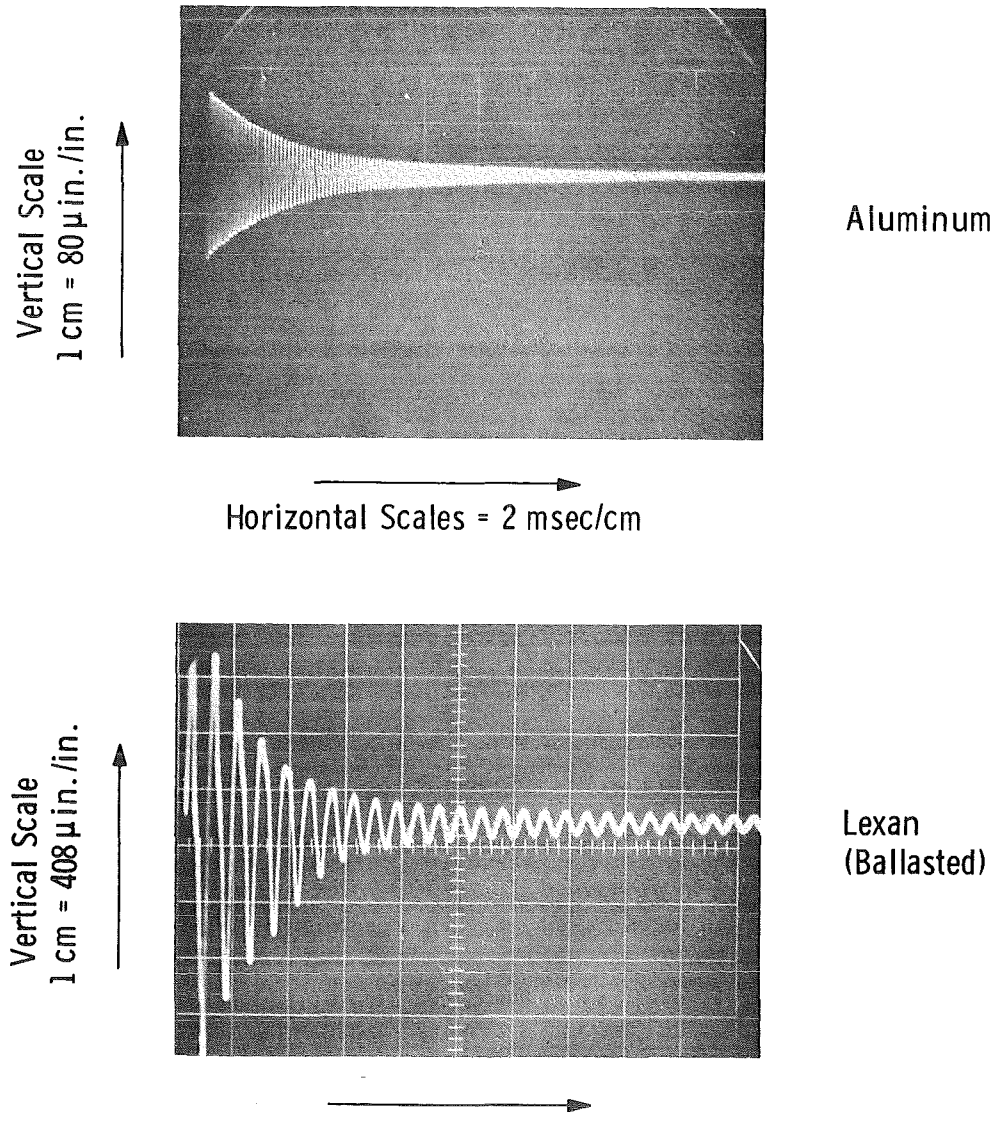

Figure 18. Vibrational response of aluminum and Lexan cones.

The oscilloscope traces were read on a film reader to determine frequency and the logarithmic decrement,

$$\Delta = (1/N)\ell_n (y_o/y_n) \tag{1}$$

In Eq. (1) N is the number of cycles, y_o is the original amplitude, and y_n is the amplitude after the N cycles. For the aluminum cone, Δ = 0.047 was obtained. The ballasted Lexan cone did not give a constant Δ. The value was lower at late times but was approximately constant at 0.3 for about 8 msec after being struck.

The calculated natural frequency of the fixed-base aluminum cone is 7960 Hz, but the measured frequency was only 6880 Hz. Part of the discrepancy may be attributed to the fact that the collar does not fully represent a fixed base for the cone. The ballasted Lexan cone experimentally yielded 1250 Hz and a wholly Lexan cone gave 2060 Hz. Therefore, rather than the computed ratio of Lexan-to-aluminum frequencies, W = 0.28, which appears in Table 3, or the experimentally determined W = 0.30, both of which apply to wholly Lexan cones, one has W = 0.18 for the ballasted Lexan cones actually used for comparison with the aluminum cones. While one cannot say if this 5.6:1 variation in cone vibrational frequency is significant in regard to boundary-layer transition under the circumstances studied, it is at least large enough to be interesting.

The time required for a given amplitude change is given by

$$\tau = [1/(\Delta f)]\ \ell_n (y_o/y_n) \tag{2}$$

where f is the frequency in Hz. Because it would seem very likely that any cone vibration is induced early within the launcher, the time elapsing between, say, the start of motion within the launcher and arrival at the viewing station is relevant insofar as the cone vibration amplitude is concerned. In the case of the Mach five experiments, this (average) time was 14.4 msec and for the Mach two launches it was 27.9 msec. Therefore, if the initial maximum amplitude, y_o, of the cone tip were known, Eq. (2) and these input data would permit a calculation of the amplitude, y_n, at the focused shadowgraph station. This calculation could not be made because y_o is not known, but an upper limit may be placed on it. For the 10-deg aluminum cone, it is calculated that a deflection of the tip of 0.065 in. would have caused the metal to yield. No such bending was ever observed in flight on 10-deg cones, so it is

safe to assume that y_o did not attain that magnitude. Assume then, as an example, $y_o \leqq 0.06$ in. Substituting into Eq. (2) the quantities

$$\tau = 14.4 \text{ msec}, \qquad f = 6880 \text{ Hz, and}$$

$$\Delta = 0.047, \qquad y_o \leqq 0.06 \text{ in.}$$

one obtains $y_n < 0.00056$ in. for the aluminum cone. Concerning the ballasted Lexan cone, using

$$\tau = 14.4 \text{ msec}, \qquad f = 1250 \text{ Hz, and}$$

$$\Delta = 0.3, \qquad y_o \leqq 3.3\ (0.06) = 0.20 \text{ in.}$$

leads to $y_n \leqq 0.00091$ in. Although the Lexan cone may start with more than three times the tip deflection of the aluminum cone, it would be expected to have roughly 1.6 times as much tip deflection at the viewing station.

Because of interest in possible higher vibrational modes, a second type of experiment was conducted with one of the 1.75-in. aluminum cones of the type actually launched. It was suspended by a string at its center of gravity and struck with a hammer. A microphone and recording system of the type used to monitor noise in the range recorded the result. Frequencies of 7680 and 7180 Hz could be identified. Higher modes could not be found by this means, and it was concluded that any higher modes were associated with very much lower amplitudes.

By this comparison of transition on aluminum and ballasted Lexan cones, one is seeing the effect of a reduction of vibrational frequency from 6880 to 1250 Hz, coupled with a corresponding increase in possible tip vibrational amplitude by a factor of 1.6. It is believed that there was a small but insignificant amount of nose tip ablation on the Lexan cones at Mach 5.0. This is discussed in the following section. Sufficient Mach five and Mach two launches have been carried out, and no significant difference in transition Reynolds numbers has been found. The Lexan cones will be identified when the transition data are discussed in Section 6.0.

It should be noted that a recent wind tunnel experiment by Olson et al. (Ref. 31) revealed no influence of model vibration on transition Reynolds number. In that situation, frequencies of 2900 to 82,000 Hz and peak-to-peak amplitudes of 40 to 1500 μin. were explored. Those authors believed that artificial roughness heights equal to the vibration amplitudes would have tripped their boundary layer, and they concluded that vibration in their case was less effective as a trip than fixed surface

roughness. Perhaps this should not be surprising. Unless a sensitive mode of vibration were chanced upon, the surface deflections owing to vibration would take the form of gentle waviness rather than abrupt discontinuities in the nature of boundary-layer trips.

5.4 NONUNIFORM WALL TEMPERATURE

A source of potential influence on transition under range conditions is the nonuniform surface temperature arising from aerodynamic heating. A hot nose will be combined with a relatively unheated afterbody, and the boundary-layer profile near the nose will reflect this. Rhudy (Ref. 32) has made an illustrative calculation of the influence of a hot leading edge section with $T_w/T_o = 0.8$ followed by a cooler plate with $T_w/T_o = 0.2$. He shows that, for $M_\delta = 6$ and $(U/\nu)_\delta = 1.1 \times 10^6$ in.$^{-1}$, it takes a distance of approximately 600 δ_j for the product ρu in the boundary layer at the critical height $y/\delta = 0.9$ to attain the profile that is calculated for a plate with $T_w/T_o = 0.2$ over its entire length. The symbol δ_j represents boundary-layer thickness at the discontinuous change of wall temperature. Apparently, there have been no experiments to investigate the seriousness of the effect of nonuniform T_w on transition prior to some recent and still unpublished work by Kendall at the Jet Propulsion Laboratory.

In the range investigations conducted by the author, calculations of stagnation point and afterbody temperatures have been made. It was calculated that Lexan cone tips would melt under the Mach five conditions and yet no decisive evidence of tip blunting was seen. Thus, it is inferred that the calculated temperature increases either were conservative or that the amount of localized ablation was too small to be seen. Inspection of the laser-lighted photographs of Lexan cones in flight revealed small decreases in length and faintly cusped tip shapes. However, the laser station was 32 percent further downrange than the principal focused shadowgraph, and ablation would have been much less at the shadowgraph where transition was determined. If one takes a published melting temperature of roughly 550°K for Lexan, it follows that the nose tips of the Lexan cones were no more than 1.8 times the temperature of the skirts which heat negligibly in the brief flight. The calculation method yields a maximum tip-to-skirt temperature ratio of roughly 2:1 for the Mach five aluminum cones as well. At Mach two, these ratios are much nearer unity.

As a conservative move, the calculated boundary-layer thickness at, say, 100 nose radii or 0.5 in. from the stagnation point may be taken as the value for Rhudy's δ_j in the present case. Then, in keeping with his results, it may be inferred that the cone boundary layers at the transition location should be essentially free of "hot-tip" influence when distance to transition, s_t, is greater than 600 δ_j. On this basis, all of the present data correspond to $s_t/\delta_j > 2000$ for the conditions encountered. Coupled with the lesser tip-to-afterbody temperature ratio and the conservative nature of this comparison with the results in Ref. 32, the hot-tip effect is not an obvious factor in the present work. Until other data are available, no more may be said.

6.0 DISCUSSION OF RESULTS

In Section 5.0 partial answers were given to some peripheral questions that concern aeroballistic data on boundary-layer transition. At its conclusion, it seems that the special features previously discussed must represent sources of boundary-layer disturbances, mostly of small magnitude and unknown impact on the transition process. There do not appear to have been any disturbances prominent enough to dominate the transition results, e.g., to have created the systematic trend of $Re_{\delta,t}$ with $(U/\nu)_\delta$. The fact that the models did oscillate, were not perfectly smooth, and did vibrate in small amplitudes may be significant in regard to sources of disturbances imposed upon and possibly amplified within the boundary layer. Perhaps it is permissible to suggest once again that all real boundary layers are disturbed in different degrees by different sources. At this time, however, evidence of any explanation of the unit Reynolds number effect arising from these factors is lacking. Therefore, the main body of data from this investigation is next presented for discussion.

6.1 TRANSITION ON SMOOTH CONES IN QUIET RANGE

Figure 19 presents the data on nominally smooth, 4- and 10-deg semiangle cones at both $M_\infty = 2.2$ and 5.1. Within the scatter of the data, no clear difference appears between the data for 4- or 10-deg cones or between the data for Mach numbers of 2.2 or 5.1. Lest one be tempted to say that no Mach number effect exists, it must be pointed out that $T_W \approx T_\infty \approx 300°K$ and that

$$T_w/T_\delta = (1 + \frac{\gamma - 1}{2} M_\delta^2)/(1 + \frac{\gamma - 1}{2} M_\infty^2)$$

Thus, on 10-deg cones,

$$T_w/T_\delta = 0.78 \text{ at } M_\infty = 5.1$$

and

$$T_w/T_\delta = 0.94 \text{ at } M_\infty = 2.2$$

On 4-deg cones at $M_\infty = 2.2$,

$$T_w/T_\delta \approx 1$$

As mentioned earlier, for 10-deg cones,

$$T_w/T_{aw} = 0.18 \text{ at } M_\infty = 5.1$$

and

$$T_w/T_{aw} = 0.50 \text{ at } M_\infty = 2.2$$

For the 4-deg cones at $M_\infty = 2.2$,

$$T_w/T_{aw} = 0.55$$

The influences of temperature levels and wall heat-transfer rates on boundary-layer transition are uncertain because of either or both conflicting data and lack of data for extreme ranges of these parameters. The general impression is that cooling the wall of a model delays transition, but there are data (Ref. 27) showing that cooling can cause earlier transition. Actually, of course, the question is much too complicated to allow an easy answer. The stability theory of Ref. 3 suggests that there is a complex interplay between different modes of instability and the heat-transfer situation existing for a particular type of disturbance at a particular Mach number.

It is relevant to this issue to call attention to the cold-wall status ($T_w << T_{aw}$) of the aeroballistic range data and the possibly important fact that the local temperature, T_δ, in the range is generally much greater than T_δ in supersonic wind tunnel cases that might be thought comparable. The point to this latter remark is that, to a good approximation,

$$\mu_1/\mu_2 = T_1^{\omega_1}/T_2^{\omega_2}$$

where μ is the absolute viscosity and ω is a function of T. Under typical aeroballistic range conditions where $T \geq 300°K$, one finds $\omega \leq 3/4$. In supersonic wind tunnels, the upper limit on ω will approach unity. Therefore, equal local values of viscosity-dependent parameters within the boundary layers are not necessarily to be expected even when $(U/\nu)_\delta$ and M_δ are equal in the cases considered.

Returning to Fig. 19, it can be seen that a large number of data points and broad range of the independent variable are desirable when working with transition data obtained from a single spark photograph of each of a series of models at random attitudes. Repetitious spark photographs of a single model at fixed, zero angle of attack have shown

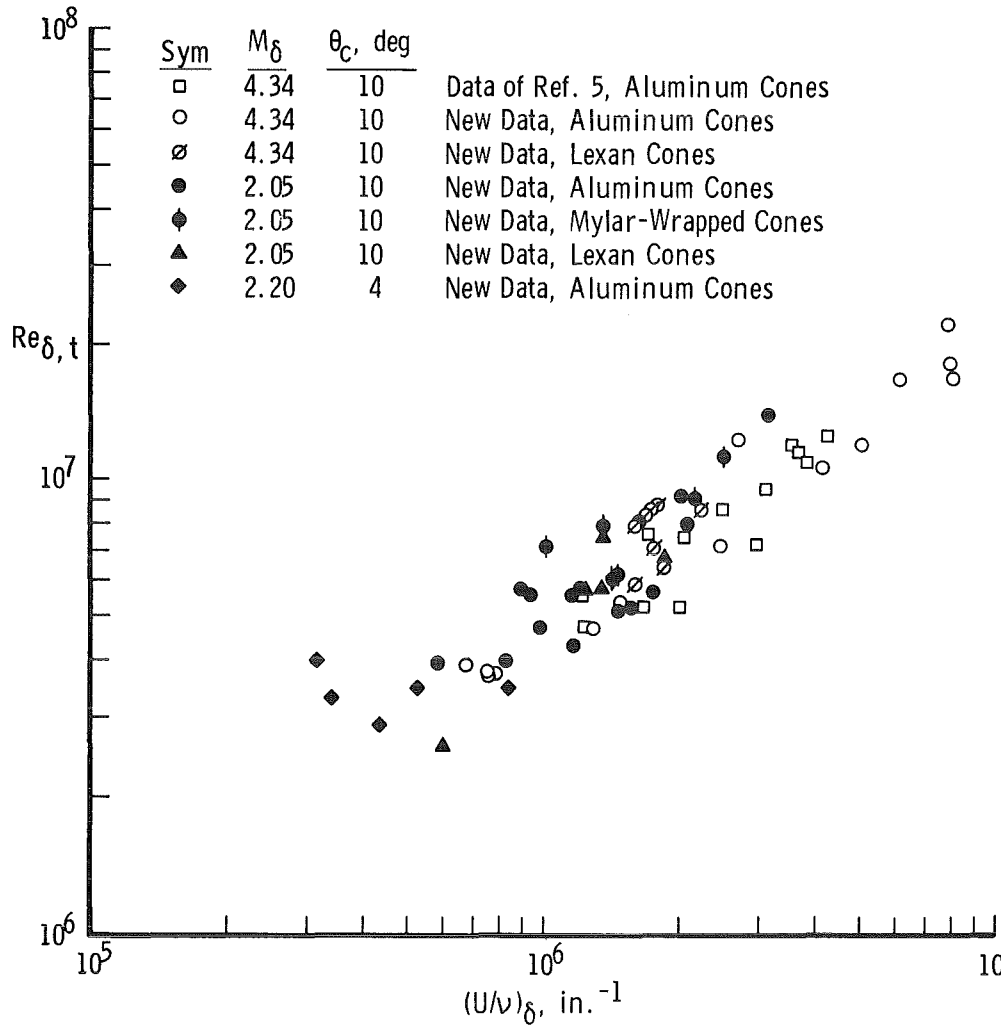

Figure 19. Smooth-cone, quiet-range transition data.

a bell-shaped or Gaussian distribution of transition locations with time (cf. Ref. 28). The near-instantaneous, single-shot photography represented in Fig. 19 certainly reflects the normal fluctuation in transition location on a given meridian of a cone, and the data spread possible may be increased by other random factors including the repeatability of the author's visual process in determining transition location in the photographs.

To conclude earlier discussion about Lexan cones and the experiment to evaluate possible cone vibration effects, the comparison of Lexan and aluminum cones is included in Fig. 19. No significant difference is apparent for either Mach number. Similarly, data from the Mylar-wrapped cones are indicated in Fig. 19, and no significant difference in results can be attributed to that refinement.

Perhaps the major message contained in Fig. 19 is that the data of Ref. 5 are supported. After extension, both in regard to $(U/\nu)_\delta$ and M_δ, the so-called unit Reynolds number effect remains strongly evident in these aeroballistic data where none of the normal wind tunnel disturbances were present. A straight-line fairing for all the data in Fig. 19 results in approximately

$$Re_{\delta,t} \; \alpha (U/\nu)_\delta^{0.65}$$

An exponent as great as 0.7 or as low as 0.6 can be defended.

6.2 OBSERVED BOUNDARY-LAYER WAVINESS

In several shadowgraphs at both Mach numbers, a pattern such as sketched below is visible at locations preceding transition.

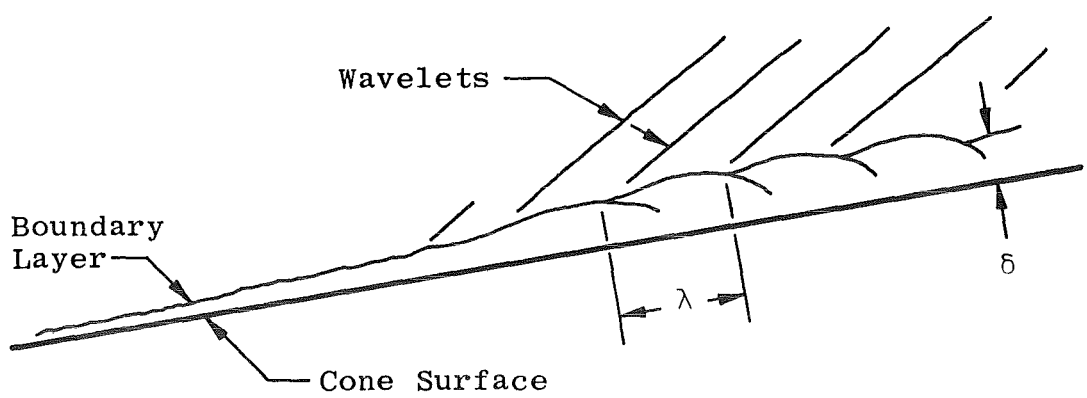

When the length, λ, is measured and compared to local boundary-layer thickness, it is found that

$$\lambda / \delta \approx 2$$

Converting to a frequency by writing U_δ / λ, where U is the inviscid-fluid, theoretical velocity on the cone surface, the result is

$$500 < U_\delta / \lambda < 600 \text{ kHz}$$

The angles of the wavelets emanating from the ripples in the boundary-layer edge appear to be very near the local Mach angle, $\sin^{-1} 1/M_\delta$. This implies that the ripples have little or no motion along the cone surface. Cone surface roughness could produce such a result, but that is not believed to be the source of the flow disturbances. Similar patterns preceding the location of transition were noted by the authors of Ref. 33 and several others since that time.

6.3 EXPERIMENT WITH NOISE INTRODUCED INTO RANGE

The normally "quiet" condition of the aeroballistic range was described in Ref. 5 and in an earlier section of this report. In an effort to perturb this condition, an available Federal Sign and Signal Corporation Model A siren was installed as near as practical to the position of free-flight cones as they passed the photographic station. Experiments with various orientations of siren and microphones showed that a 130-db field was introduced in the area of the model by this means. The peak amplitude of the fluctuating sound pressure level, normalized by the range static pressure most used for this phase of the study was

$$\tilde{p}/p_\infty \approx 4.7 \times 10^{-4}, \text{ rms}$$

for 40-Hz to 40-kHz frequencies, and the dominant frequency of the near-sinusoidal waveform was 800 Hz. A Bruel and Kjaer 1/2-in. Model 4133 microphone was used for these measurements.

For comparison, it may be noted that sound pressure ratios mentioned in Ref. 9 for a wind tunnel at Mach three conditions are

$$0.014 < \tilde{p}/p_\infty < 0.035 \text{ rms}$$

Thus, while the siren produced an rms level of $\tilde{p}/p_\infty$ more than 200 times greater than the measured maximum in the "quiet" range, the

ratio remained an order of ten less than would be expected in a typical supersonic wind tunnel. (Note that these ratios are different if $\tilde{p}$ rather than $\tilde{p}/p_\infty$ is the basis of comparison.)

Figure 20 presents results for several cones launched with the siren operating. Static pressure, p_∞, was 1040 mm Hg for the 10-deg cones at Mach two and 239 mm Hg for the 4-deg cone at Mach two. The 10-deg cones at Mach five were launched with 450 mm Hg. It is clear that the particular noise spectrum imposed by the siren did not produce a significant effect on boundary-layer transition. The low frequency of the siren output could be the cause of this, but it is noteworthy that sound pressure ratio, even with the siren, was still very low in comparison to supersonic tunnel test sections.

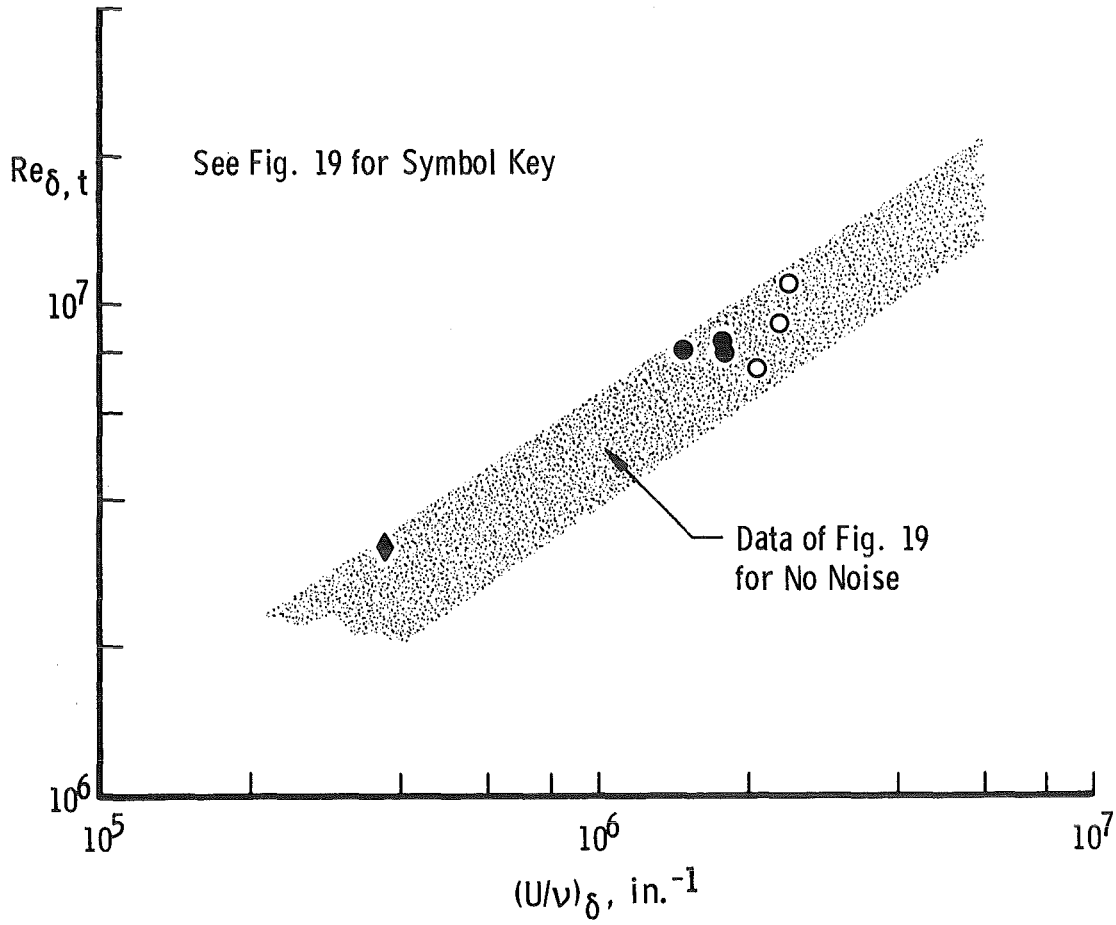

Figure 20. Influence of elevated noise level on transition reynolds number.

7.0 CONCLUDING REMARKS

The principal conclusion is that a form of "unit Reynolds number effect" seems to exist in the free-flight range environment. None of the range-peculiar conditions investigated thus far appear to offer an explanation for this result which now is shown to exist at two supersonic Mach numbers. The introduction of noise in the form of 800-Hz, 130-db siren output failed to measurably affect transition Reynolds numbers. The particular conditions of the latter experiment, which was performed with available equipment, may not have been appropriate for producing a large effect. The mildly surprising equality of Reynolds numbers of transition at $M_\delta \approx 2.1$ and 4.3, with $T_W = T_\infty = 300°K$ in both cases, deserves further investigation. Whether or not the different wall temperature ratios, T_W/T_{aw}, compensated for Mach number effect remains a question.

REFERENCES

1. Morkovin, M. V. "Critical Evaluation of Transition from Laminar to Turbulent Shear Layers with Emphasis on Hypersonically Traveling Bodies." AFFDL-TR-68-149, 1968.
2. Morkovin, M. V. In Viscous Drag Reduction, Plenum Press, New York, 1969, pp. 1-31.
3. Mack, L. M. "Boundary Layer Stability Theory." Jet Propulsion Laboratory JPL 900-277 Rev. A, November 1969.
4. Mack. L. M. and Morkovin, M. V. AIAA short course notes on boundary-layer stability and transition, New York, 1969.
5. Potter, J. L. "Observations on the Influence of Ambient Pressure on Boundary-Layer Transition." AIAA Journal, Vol. 6, No. 10, October 1968, pp. 1907-1911.
6. Reshotko, E. "Stability Theory as a Guide to the Evaluation of Transition Data." AIAA Journal, Vol. 7, No. 6, June 1969, pp. 1086-1091.
7. Ross, R. "Influence of Total Temperature on Transition in Supersonic Flow." AIAA Journal, Vol. 11, No. 4, April 1973, pp. 563-565.

8. Laufer, J. "Aerodynamic Noise in Supersonic Wind Tunnels." Journal of the Aerospace Sciences, Vol. 28, No. 9, September 1961, pp. 685-692.

9. Pate, S. R. and Schueler, C. J. "Radiated Aerodynamic Noise Effects on Boundary Layer Transition in Supersonic and Hypersonic Wind Tunnels." AIAA Journal, Vol. 7, No. 3, March 1969, pp. 450-457.

10. Schlichting, H. Boundary Layer Theory. Translated by J. Kestin, 4th ed., McGraw-Hill, New York, 1960, pp. 439-445.

11. Liepmann, H. W. "Investigations on Laminar Boundary Layer Stability and Transition on Curved Boundaries." NACA ACR No. 3H30, August 1943.

12. Persen, L. N. "Investigation of Streamwise Vortex Systems Generated in Certain Classes of Curved Flow." Part I, ARL 68-0134, July 1968.

13. Persen, L. N. "Investigation of Streamwise Vortex Systems Generated in Certain Classes of Curved Flow." Part II, ARL 68-0133, July 1968.

14. Persen, L. N. "Investigation of Streamwise Vortex Systems in Curved Flow." ARL 70-0156, September 1970.

15. Persen, L. N. "Exploratory Experiments in Water on Streamwise Vortices and Crosshatching of the Surface of Reentry Bodies." ARL 69-0160, September 1969.

16. Görtler, Heinrich. "Dreidimensionale Instabilität der ebenen Staupunktströmung gegenüber wirbelartigen Störungen." pp. 304-314, in Görtler, H. and Tollmien, W., eds. 50 [Fünfzig] Jahre Grenzschichtforschung. Braunschweig: Frederick Vieweg und Sohn, 1955.

17. Miller, J. A. and Fejer, A. A. "Transition Phenomena in Oscillating Boundary Layer Flows." Journal of Fluid Mechanics, Vol. 18, Part 3, March 1964, pp. 438-448.

18. Laufer, J. and Vrebalovich, T. "Stability and Transition of a Supersonic Laminar Boundary Layer on an Insulated Flat Plate." Journal of Fluid Mechanics, Vol. 9, Part 2, February 1960, pp. 257-299.

19. Fahy, F. J. and Pretlove, A. J. "Acoustic Forces on a Flexible Panel Which Is Part of a Duct Carrying Air Flow." Journal of Sound and Vibration, Vol. 5, No. 2, February 1967, pp. 302-316.

20. Fischer, M. C. and Rudy, D. H. "Effect of Angle of Attack on Boundary-Layer Transition at Mach 21." AIAA Journal, Vol. 9, No. 6, June 1971, pp. 1203-1205.

21. Stetson, K. F. and Rushton, G. H. "Shock Tunnel Investigation of Boundary-Layer Transition at M = 5.5." AIAA Journal, Vol. 5, No. 5, May 1967, pp. 899-906.

22. Fischer, M. C. "An Experimental Investigation of Boundary Layer Transition on a 10° Half-Angle Cone at Mach 6.9." NASA TN D-5766, 1970.

23. Stainback, P. C. "Effect of Unit Reynolds Number, Nose Bluntness, Angle of Attack and Roughness on Transition on a 5° Half-Angle Cone at Mach 8." NASA TN D-4961, 1969.

24. DiCristina, V. "Three-Dimensional Laminar Boundary-Layer Transition on a Sharp 8° Cone at Mach 10." AIAA Journal, Vol. 8, No. 5, May 1970, pp. 852-856.

25. Ward, L. K. "Influence of Boundary Layer Transition on Dynamic Stability at Hypersonic Speeds." Transactions of the Second Technical Workshop on Dynamic Stability Testing, Arnold Engineering Development Center, Vol. II, April 1965 (AD472298).

26. Kendall, J. M., Jr. "Wind Tunnel Experiments on Fluctuation Sources and Amplification Rates in Supersonic and Hypersonic Boundary Layers." AIAA Paper 74-133, February 1, 1974.

27. Mateer, G. C. "Effects of Wall Cooling and Angle of Attack on Boundary Layer Transition on Sharp Cones at $M_\infty = 7.4$." NASA TN D-6908, August 1972.

28. Potter, J. L. and Whitfield, J. D. "Effects of Slight Nose Bluntness and Roughness on Boundary-Layer Transition in Supersonic Flows." Journal of Fluid Mechanics, Vol. 12, Part 4, 1962, pp. 501-535.

29. Wilkins, M. E. and Darsow, J. F. "Finishing and Inspection of Model Surfaces and Boundary-Layer-Transition Tests." NASA Memo 1-19-59A, February 1959.

30. Dugger, P. H., Enis, C. P., and Hill, J. W. "Laser High-Speed Photography for Accurate Measurements of the Contours of Models in Hypervelocity Flight within an Aeroballistic Range." Proceedings of the Technical Program, Electro-Optical Systems Design Conference, New York, September 1970.

31. Olson, L. E., Gregorek, G. M., and Lee, J. D. "The Influence of Artificially Induced Turbulence upon Boundary-Layer Transition in Supersonic Flows." Aerospace Research Labs ARL 71-0022, January 1971.

32. Rhudy, J. P. "Effect of Uncooled Leading Edge on Cooled-Wall Hypersonic Flat-Plate Boundary-Layer Transition." AIAA Journal, Vol. 8, No. 3, March 1970, pp. 576-577.

33. Potter, J. L. and Whitfield, J. D. "Boundary Layer Transition Under Hypersonic Conditions." AEDC-TR-65-99 (AD462716), May 1965.

NOMENCLATURE

c_r	Phase velocity of disturbance = velocity of wave propagation in free-stream direction
f	Frequency of vibration of cone
k	Roughness element depth as measured by profilometer
M	Mach number
N	Number of cycles of vibration
p	Pressure
$\tilde{p}$	Fluctuating sound pressure amplitude
Re	Reynolds number
s	Distance measured along surface from stagnation point
T	Temperature
U	Velocity
α	Total angle of attack; also designates "proportional to"
α_p	Angle of attack in plane of photograph

β	Characteristic angular frequency of disturbance spectrum
γ	Ratio of specific heats
δ	Boundary-layer thickness
θ	Characteristic orientation of disturbance spectrum
θ_c	Cone semiapex angle
λ	Characteristic wavelength of disturbance spectrum
μ	Absolute viscosity
ν	Kinematic viscosity = μ/ρ
ρ	Mass density
ϕ	Orientation of a cone meridian relative to the windward "stagnation line" where $\phi = 0$
ω	Exponent in the approximation $\mu \propto T^{\omega}$

SUBSCRIPTS

aw	Adiabatic wall
o	Total, e.g., total temperature; also designates $\alpha = 0$
t	Transition
w	Cone wall
α	Denotes $\alpha \neq 0$
δ	Local flow parameter at outer edge of boundary layer
∞	Free stream